Tran-SET

Transportation Consortium of South-Central States

Solving Emerging Transportation Resiliency, Sustainability, and Economic Challenges through the Use of Innovative Materials and Construction Methods: From Research to Implementation

Real-Time Early Detection and Monitoring of Flooding Using Low-Cost Highly Sensitivity Ultrasound Sensing of Water Level

Project No. 19ASUTA03

Lead University: the University of Texas at Arlington

Final Report

August 2020

Disclaimer

The contents of this report reflect the views of the authors, who are responsible for the facts and the accuracy of the information presented herein. This document is disseminated in the interest of information exchange. The report is funded, partially or entirely, by a grant from the U.S. Department of Transportation's University Transportation Centers Program. However, the U.S. Government assumes no liability for the contents or use thereof.

Acknowledgements

The authors acknowledge the Tran-SET for providing the financial support of this study. The authors also would like to thank Project Review Committees, Trent Ballard, Kyu jung Kim, and Do Soo Moon for their supports and directions of the project.

TECHNICAL DOCUMENTATION PAGE

1. Project No.	2. Government Accession No.	3. Recipient's Catalog No.
19SAUTA03		

4. Title and Subtitle	5. Report Date
Real-Time Early Detection and Monitoring of Flooding Using Low-Cost Highly Sensitivity Ultrasound Sensing of Water Level	Aug. 2020
	6. Performing Organization Code
7. Author(s) PI: Dr. Suyun Ham (ORCID: 0000-0001-6375-211X) Co-PI: Dr. Seongjin Noh (ORCID: 0000-0002-2683-7269) Co-PI: Dr. Dong-Jun Seo (ORCID: 0000-0003-3863-8408) GRA: Sanggoo Kang GRA: Dafnik Saril Kumar David	**8. Performing Organization Report No.**
9. Performing Organization Name and Address Transportation Consortium of South-Central States (Tran-SET) University Transportation Center for Region 6 3319 Patrick F. Taylor Hall, Louisiana State University, Baton Rouge, LA 70803	**10. Work Unit No. (TRAIS)**
	11. Contract or Grant No. 69A3551747106
12. Sponsoring Agency Name and Address United States of America Department of Transportation Research and Innovative Technology Administration	**13. Type of Report and Period Covered** Final Research Report Aug. 2019 – Aug. 2020
	14. Sponsoring Agency Code

15. Supplementary Notes

Report uploaded and accessible at Tran-SET's website (http://transet.lsu.edu/).

16. Abstract

Flooding poses safety hazards to motorists, emergency and maintenance crews and may cause costly damage to transportation infrastructure and its operation. Flash flooding, in particular, causes the most flood-related deaths According to NOAA, in 2017 alone, flash flooding also caused $60.7 billion worth of economic damage. Low-water crossings are among the first places where deaths and significant damages to vehicles occur during flooding. With flash flooding, when a critical corridor is blocked by a high level of water, it affects the safety of the general public. To keep the critical corridors open as long as possible, and to minimize losses from flooding, accurate early detection of the rising water level is essential. The flood level detection system has to have flood stage maps in the geographic information system for the street-, roadway-, and critical-freight corridors. This area encompasses public roads in urbanized areas that provide access and connection to the primary roads for ports, public transportation or other transportation facilities. The main goal of this project is to develop cost-effective and high efficient solar-powered water level detection units and implement real-time water level monitoring for water both pavement and river stream. The project was performed with three objectives: to develop the low cost reliable real-time data of the ultrasound water level detection system, increasing its data reliability and resolution; 2) to improve an energy-saving processing system; and to deploy the ultrasound water level detection system and real-time monitoring system for water both pavement and river stream for safety measures. The obtained results and findings imply the developed monitoring system can present reliable water level data with efficient power and data transmission system.

17. Key Words	18. Distribution Statement
Ultrasound water level detection system, real-time monitoring, microcontroller, cloud computing platform, flood monitoring	No restrictions. This document is available through the National Technical Information Service, Springfield, VA 22161.

19. Security Classif. (of this report)	20. Security Classif. (of this page)	21. No. of Pages	22. Price
Unclassified	Unclassified	41	

Form DOT F 1700.7 (8-72) **Reproduction of completed page authorized.**

SI* (MODERN METRIC) CONVERSION FACTORS

APPROXIMATE CONVERSIONS TO SI UNITS

Symbol	When You Know	Multiply By	To Find	Symbol
		LENGTH		
in	inches	25.4	millimeters	mm
ft	feet	0.305	meters	m
yd	yards	0.914	meters	m
mi	miles	1.61	kilometers	km
		AREA		
in^2	square inches	645.2	square millimeters	mm^2
ft^2	square feet	0.093	square meters	m^2
yd^2	square yard	0.836	square meters	m^2
ac	acres	0.405	hectares	ha
mi^2	square miles	2.59	square kilometers	km^2
		VOLUME		
fl oz	fluid ounces	29.57	milliliters	mL
gal	gallons	3.785	liters	L
ft^3	cubic feet	0.028	cubic meters	m^3
yd^3	cubic yards	0.765	cubic meters	m^3
		NOTE: volumes greater than 1000 L shall be shown in m^3		
		MASS		
oz	ounces	28.35	grams	g
lb	pounds	0.454	kilograms	kg
T	short tons (2000 lb)	0.907	megagrams (or "metric ton")	Mg (or "t")
		TEMPERATURE (exact degrees)		
^oF	Fahrenheit	5 (F-32)/9 or (F-32)/1.8	Celsius	^oC
		ILLUMINATION		
fc	foot-candles	10.76	lux	lx
fl	foot-Lamberts	3.426	$candela/m^2$	cd/m^2
		FORCE and PRESSURE or STRESS		
lbf	poundforce	4.45	newtons	N
lbf/in^2	poundforce per square inch	6.89	kilopascals	kPa

APPROXIMATE CONVERSIONS FROM SI UNITS

Symbol	When You Know	Multiply By	To Find	Symbol
		LENGTH		
mm	millimeters	0.039	inches	in
m	meters	3.28	feet	ft
m	meters	1.09	yards	yd
km	kilometers	0.621	miles	mi
		AREA		
mm^2	square millimeters	0.0016	square inches	in^2
m^2	square meters	10.764	square feet	ft^2
m^2	square meters	1.195	square yards	yd^2
ha	hectares	2.47	acres	ac
km^2	square kilometers	0.386	square miles	mi^2
		VOLUME		
mL	milliliters	0.034	fluid ounces	fl oz
L	liters	0.264	gallons	gal
m^3	cubic meters	35.314	cubic feet	ft^3
m^3	cubic meters	1.307	cubic yards	yd^3
		MASS		
g	grams	0.035	ounces	oz
kg	kilograms	2.202	pounds	lb
Mg (or "t")	megagrams (or "metric ton")	1.103	short tons (2000 lb)	T
		TEMPERATURE (exact degrees)		
^oC	Celsius	1.8C+32	Fahrenheit	^oF
		ILLUMINATION		
lx	lux	0.0929	foot-candles	fc
cd/m^2	$candela/m^2$	0.2919	foot-Lamberts	fl
		FORCE and PRESSURE or STRESS		
N	newtons	0.225	poundforce	lbf
kPa	kilopascals	0.145	poundforce per square inch	lbf/in^2

TABLE OF CONTENTS

LIST OF FIGURES

LIST OF TABLES

ACRONYMS, ABBREVIATIONS, AND SYMBOLS

API	Application Programming Interface
AWS	Amazon Web Service
COP	Computer Operating Properly
EC2	Elastic Compute Cloud
GPS	Global Positioning System
GIS	Geographic Information System
HTML	Hypertext Markup Language
IMEI	International Mobile Equipment Identify
MCU	Microcontroller
NOAA	National Oceanic Atmospheric Administration
RTC	Real-Time Clock
SSR	Solid State Relay
SRAM	Static Random Access Memory
TXDOT	Texas Department of Transportation
UWLD	Ultrasonic Water Level Detection
UAV	Unmanned Aerial Vehicles
UTA	University of Texas at Arlington

EXECUTIVE SUMMARY

Flooding poses safety hazards to motorists, emergency, and maintenance crews and may cause costly damage to transportation infrastructure and its operation. Flash flooding, in particular, causes the most flood-related deaths. According to National Oceanic and Atmospheric Administration (NOAA), in 2017 alone, flash flooding also caused $60.7 billion worth of economic damage. Low-water crossings are among the first places where deaths and significant damages to vehicles occur during flooding. With flash flooding, when a critical corridor is blocked by a high level of water, it affects the safety of the general public. To keep the critical corridors open as long as possible, and to minimize losses from flooding, accurate early detection of the rising water level is essential. The flood level detection system has to have flood stage maps (i.e., normal or extreme water elevation) in the geographic information system (GIS), for the street-, roadway-, and critical-freight corridors. This area is encompassing public roads in urbanized areas that provide access and connection to the primary roads for ports, public transportation, or other transportation facilities. The traffic will exhibit both commuter and freight congestion. The critical corridors are a high priority in Texas Freight Mobility Plan 2017.

Water level detection units are commonly designed for riverine flooding rather than flash flooding. Moreover, installation and maintenance of traditional water level sensing systems are expensive (> $ 75,000). The current cutting-edge water level detection techniques, on the other hand, have significant limitations: noise and erroneous signals from sensors, unstable power management, and slow data transmitting. Unmanned aerial vehicles (UAV) may also be used to sense flash floods in real-time. The UAVs, however, have their limitations in that they only provide snapshots of flood information in the short period of time they operate.

As a promising solution, this study will evaluate a low-cost real-time ultrasound water-level measuring unit at critical corridors in Region 6, to develop integrated-sensing of the low-cost, highly sensitive ultrasound water level detection (UWLD) unit to increase its reliability and resolution and to integrate it with a highly efficient solar power system and a reliable cellular network. The flood stage information will be transmitted using a cellular module in the UWLD unit to the Region 6 Flood Control District or sent directly to emergency command centers for an early warning so that they may take timely action such as citizen/driver evacuation, route/ramp closures, and signal timing modification.

The educational impact of this project is that sensing and monitoring elements of the research is integrated into a planned graduate-level course: "Advanced sensing and monitoring." This research is highly interdisciplinary and engaged students from multiple departments (i.e., civil engineering, computer science, electrical engineering). This project's novel technologies will help develop new skill sets for the workforce that is most involved with roadway safety and direction during flooding. The PI developed several training and outreach programs at the University of Texas at Arlington (UTA). Other information is disseminated at conferences and papers dedicated to this topic. In the future, the research team will invite leaders from companion programs to UTA for seminars. He will also consult with Region 6 DOT concerning the best way to contact state leaders who are open to meetings with those who could best use this technology.

1. INTRODUCTION

Flooding poses safety hazards to motorists, emergency and maintenance crews and may cause costly damage to transportation infrastructure and its operation. Flash flooding, in particular, causes the most flood-related deaths *(1, 2)*. According to NOAA, in 2017 alone, flash flooding also caused $60.7 billion worth of economic damage. Low-water crossings are among the first places where deaths and significant damages to vehicles occur during flooding. With flash flooding, when a critical corridor is blocked by a high level of water, it affects the safety of the general public. To keep the critical corridors open as long as possible and to minimize losses from flooding, accurate early detection of the rising water level is essential. The flood level detection system has to have flood stage maps (i.e., normal or extreme water elevation) in the geographic information system (GIS), for the street-, roadway-, and critical-freight corridors *(3)*. This area encompasses public roads in urbanized areas that provide access and connection to the primary roads for ports, public transportation, or other transportation facilities. The traffic will exhibit both commuter and freight congestion. The critical corridors are a high priority in Texas Freight Mobility Plan 2017 *(4)*.

Water level detection units are commonly designed for riverine flooding rather than flash flooding. Moreover, installation and maintenance of traditional water level sensing systems are expensive (> $ 75,000). The current cutting-edge water level detection techniques, on the other hand, have significant limitations: noise and erroneous signals from sensors, unstable power management, and slow data transmitting.

The ultrasound-based approach is one of the most advanced water level monitoring systems. In spite of that, the current flash flood water level system with the sensing and other similar techniques exhibit drawbacks with several major practical issues: low accuracy, unstable power management issue, and dependency of stream water level. The low accuracy of at best 15 mm can be challenged to precisely provide information on extreme weather conditions. In addition, signal loss due to power management issues and inappropriate signal processing due to the intrinsic nature of the sensor (e.g., wave scattering) also may cause the drawbacks. These unexpected noises and error may mistakenly issue a false flash flood warning from the Emergency Alert System. Meanwhile, due to the inaccuracy of the current ultrasound system, there have been few efforts to monitor and warn water levels on transportation roads and low-crossing bridges, if possible, in real-time. The challenges to having real-time reliable water level monitoring are to develop the low-cost, highly sensitive ultrasonic water level detection (UWLD) system, which is transferable to the database accessible in real-time and secures the stable operation of UWLD system covering both pavement and riverine.

2. OBJECTIVES AND APPROACH

2.1 Objective

The main goal of this project is to develop cost-effective and high efficient solar-powered water level detection units and implement real-time water level monitoring for water both pavement and river stream. Three objectives are proposed:

- Objective 1: the first objective is to develop the low cost reliable real-time data of the UWLD system, increasing its data reliability and resolution. The UWLD system unit is developed with cost-effective components, reliable water level measurement system, and real-time data transmission and monitoring system using a cloud computing platform. To obtain the reliable UWLD data, proper data collecting interval and filter are considered.
- Objective 2: the second objective is to improve an energy-saving processing system. The stable power supply by the developed unit itself is significant to operate the sensor and other components controlled by microcontrollers (MCUs).
- Objective 3: the last objective is to deploy the UWLD system and real-time monitoring system for water both pavement and stream for safety measures.

2.2 Approach and Literature Review

Natural disasters (e.g., floods) often lead to loss of lives and properties in many years. Particularly, urban flash floods are critically dangerous, due to its short times of event in the population density of cities. The challenge is that there is a lack of information on the threatening flood (type, location, and severity), sensing these events is important to generate accurate and detailed flashflood warnings. The water level detecting sensors have been investigated for the flood monitoring (*5*), in particular its on bridges (*6*), or pressure sensors of water level detection on rivers (*7*). Indeed, these sensors are unable to measure the dynamic pressures independently and are affected by their orientation with respect to the water flow. Ultrasound rangefinder, which allows measuring the distance between the object and sensor, was adopted for the flood level monitoring (*8*). In this paper, a sensing device is deployed to monitor urban flash floods combining ultrasonic range finding with remote temperature sensing. The example of the distance data from the ultrasound transducer is shown at the top of Figure 1.

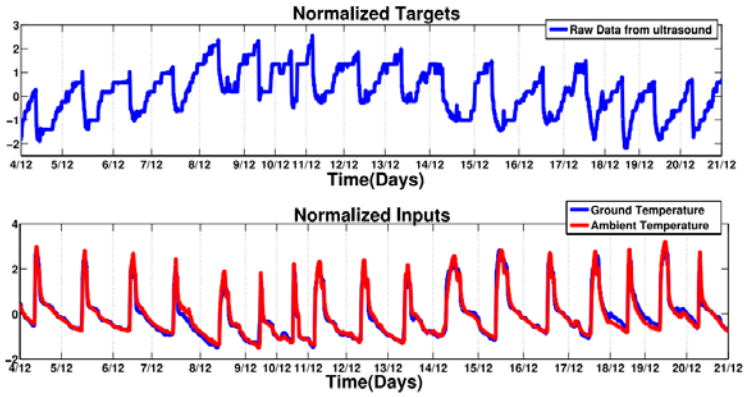

Figure 1. Example of the distance data from the ultrasound sensor and temperature data (8)

The distance measurement based on the two-way travel time of the ultrasound, which is traveled in the air medium, is influenced by the temperature. The ultrasound wave velocity in the dry air is given approximately by Equation 1 (*9*).

$$v_{sound\ in\ air} \approx 331.4 + 0.6T_c\ (m/s) \qquad [\ 1\ ]$$

where $v_{sound\ in\ air}$ = wave velocity in the air and T_c = Celsius temperature

The unit is based on distance sensing using an ultrasound transducer and reliable cellular data transmission. Non-contact ultrasonic detections have been selectively used depending on the target, such as distance detection and damage identification (*10–12*).

To obtain reliable distance data, moving average data filtering have processed (*8*). The moving average filtering is used with time series data to smooth out short-term fluctuations. The most basic way to use the moving average is a simple moving average (SMA), which uses the average value calculated from multiple measurements to smooth out the fluctuation, as Equation 2 (*13*).

$$D = \frac{\sum_1^n MD_i}{n} \qquad [\ 2\ ]$$

where *D* is depth, MD_i is i^{th} measured depth, *n* is the number of the measurement.

In case there is an outlier value that is extremely far from the other values, the value should be excluded from the consideration instead of including in the average calculation. But these outlier values are included in the calculation when moving average filter is used, which haves the moving average filter too sensitive to outlier values. So, a different filter should be selected, and a moving median filter will be the one. In moving the median filter, the median value will be chosen from multiple measurements to leave out the noise. In moving median filter, the outlier values can be excluded from consideration as the following (*14*)

$$D = MD_k; \quad k = \frac{(n+1)}{2} \qquad (n \text{ odd}) \qquad [\ 3\ ]$$

$$D = \frac{MD_k + MD_l}{2}; \quad k = \frac{n}{2}; \quad l = \frac{n}{2} + 1 \qquad (n \text{ odd}) \qquad [\ 4\ ]$$

The real-time flood monitoring has been developed with open source data-sharing network (*15*) and cloud computing platform (*16*, *17*). Although there are many studies of water level detection techniques, they have significant limitations: noise and erroneous signals from sensors, unstable power management, and slow data transmitting.

3. PROCEDURE

3.1. Ultrasound water level detection system

The ultrasonic water level detection (UWLD) system was developed to perform low-cost and highly sensitive water level detection and to provide reliable real-time monitoring data. In this system, measured distance values between ultrasound sensor and water surface are processed to the water level data considering ultrasound wave speed changes by temperature. The processed water level data is transferred to the AWS server for the real-time monitoring of the water level at the node.

3.1.1. UWLD System with Internal Sleep Mode using a Computer-Operating-Properly Timer

The UWLD system can be summed up in three steps: 1) collecting distance and temperature data, 2) calculating water level, and 3) sending the data to the AWS server in real-time. The unit of the system consists of a microcontroller (MCU), an ultrasound range or distance sensor, a cellular module, a solar panel, a battery charger, and a battery. The system is designed with components that are connected as the system representation is illustrated in Figure 2.

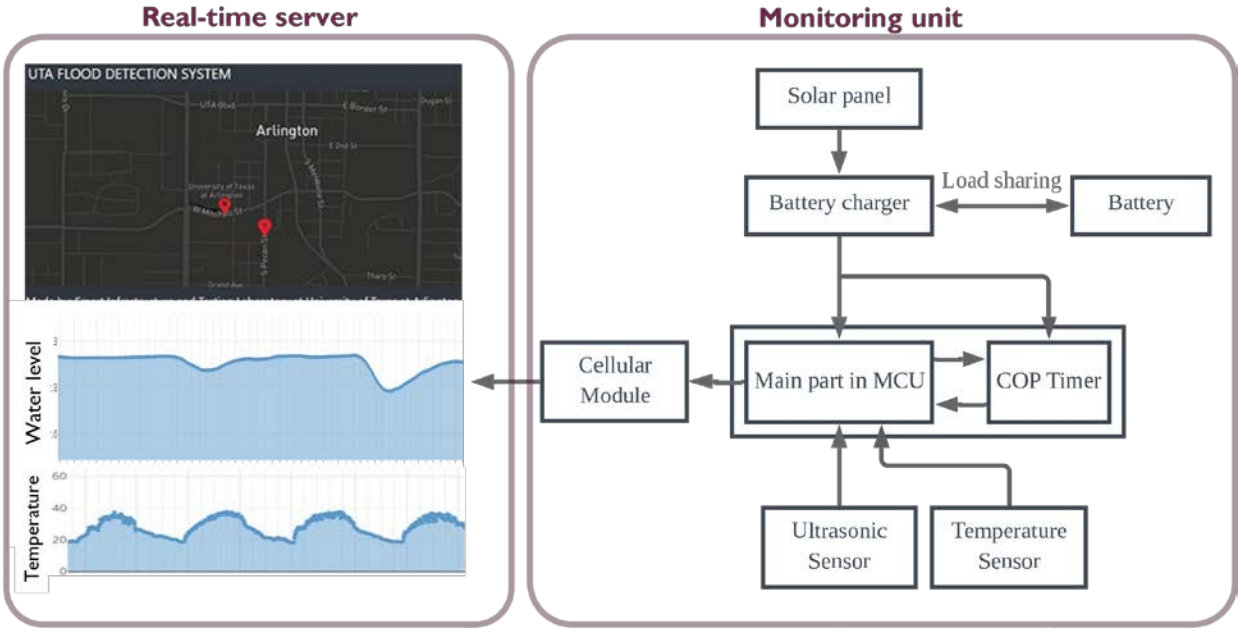

Figure 2. System representation of the UWLD system.

In the first step, for efficient power-management, a proper interval time should be located after sending the data step and before collecting data step in the next cycle. As the system collects data, the system may be turned off unintentionally due to the low energy or battery level during the rainy season when there is not enough sunlight to charge the battery. It is highly important to employ interval time for battery sustainability after sending the monitoring data step and before collecting data step in the next cycle. At the first design, a sleep mode was initially employed in the interval time to provide a power-saving state. This is the simplest way for energy-saving. A computer operating properly (COP) timer controls the MCU to attain a power-saving state and to re-operate the system. The COP timer works like an alarm clock, as referred to as watchdog. When certain

sleep time is given from the code, the COP timer turns off all other parts and turns on them again after a certain sleep duration. All operation steps (e.g., collecting data, sending data, and interval time) of the flowchart in the system are described in Figure 3. From the flowchart, two decision points are employed for the high stability of the UWLD operation. Decision 1 in the figure is for checking whether the cellular module is connected well. And Decision 2 is for checking the completion of one cycle of collecting and sending data within 1 minute. The one cycle is normally completed within 30 seconds, so it means an error occurs if the cycle is not completed within 1 minute. And the watchdog timer allows rebooting the system when an error occurs. The timer is normally included in Atmel's MCU to automatically reset an embedded device.

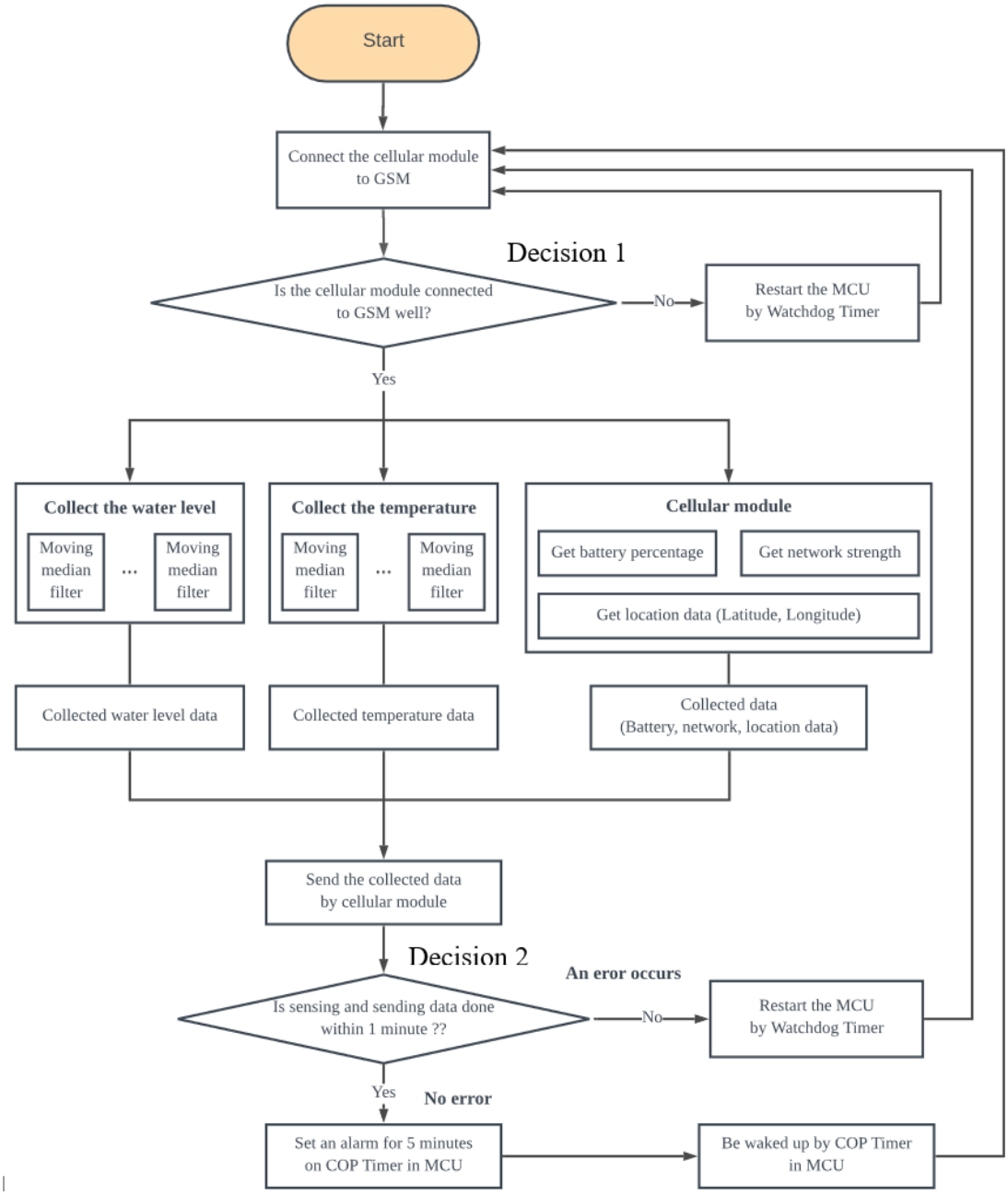

Figure 3. Data flow algorithm of the UWLD system

Two sensors, an ultrasound distance sensor, and a temperature sensor are deployed to collect distance between the sensor and water surface and temperature data. Measured distance values from the installed unit at the node are processed to obtain the water level distance by calculating the two way travel time based on the ultrasound wave speed modified by the measured temperature at the second step. For the last step, the cellular module is operated to transfer the data collected by sensors to the AWS server for real-time data plotting. The battery charging and power supply system with a solar panel, battery charger, and the battery is deployed for a stable power supply to the MCU and sensors. The battery charger has a load-sharing function that allows the solar panel to charge the battery and supply power to the MCU and sensors simultaneously (note Figure 1). Charger with this function is deployed for daytime when the solar panel produces more electricity than it is needed for operating the UWLD system.

The moving median filter (note Figure 2) is used to collect reliable distance date by choosing the median distance value among the series of distance data. It is because two different errors are mostly presented with minimum and maximum value of the ultrasound distance sensor range (minimum value error: when the object block the wave lower than sensor range, maximum value error: when the sensor loses the reflected ultrasound wave). If the series of measured distance data includes this type of error, the moving averaged method shows unreliable distance with the actual distance. The multiple measured distances are sorted in ascending order, and the median distance is chosen as the distance value at the moment.

3.1.2. Real-time AWS sever

To monitor the water level data in real-time, the online accessible cloud computing platform is used. The website to display the transferred data from UWLD was created in Amazon Elastic Compute Cloud (EC2), which can build the website and store the database as a part of AWS. The transferred data from the UWLD system consists of water level, temperature, battery percentage, current network strength, location data (GPS data) with international mobile equipment identify (IMEI) number. The location of nodes is marked on the map with an application programming interface (API). The unit location can be present with the mark on the map, and the more detailed information of the node comes up when the red mark is clicked (see Figure 2 (left)). Table 1 describes the database information, which includes all the data transferred from the UWLD system and given by the computing platform.

UWLD unit transfers the measured data to the AWS database, which can be developed and accessed by the programming language MySQL. "Database" created are shown in Table 1 with three databases: *Device, Device Table,* and *Water Data*. *Device Table* consists of all the data, whereas the remaining other two databases (Device and Water Data) have only a few parameters to reduce the processing time in the server. Database checks the IMEI number of the unit and creates a new database if it is the new UWLD unit. The flood level monitoring website based on the programming language of HTML is designed with a user-friendly interface by displaying the real-time graphs. JavaScript programming language is used to communicate between database and website with NodeJS, ReactJS, and ExpressJS languages. NodeJS allows to access the database with the data type structure (see Figure 4). ReactJS gives actions to process the data after accessing the database. ExpressJS is used for the visualization of the data in the HTML website.

Since there are many programming languages, application programming interface (API) is required to interact between the actions in the data flow Figure 4. Finally, the website deploys the virtual map with the latitude and longitude information of the UWLD unit obtained from API

device records, which consists of the device ID. The UWLD data linked to the device ID is presented in the graph format after the filtering and correcting. In addition, the data set is available for download in CSV file format.

Table 1. Database information of AWS sever

Database Name	Database information
Device	It consists of the data set of IMEI number, Latitude, Longitude, Status and Device ID
Device Table	It consists of the data set of IMEI number, Latitude, Longitude, Status, Sidewalk depth, Stream depth, Temperature, Network Strength, Battery Status and Device ID
Water Data	It consists of the data set of IMEI number, Sidewalk depth, Stream depth, Latitude, Longitude, Temperature, Battery Status, and Device ID

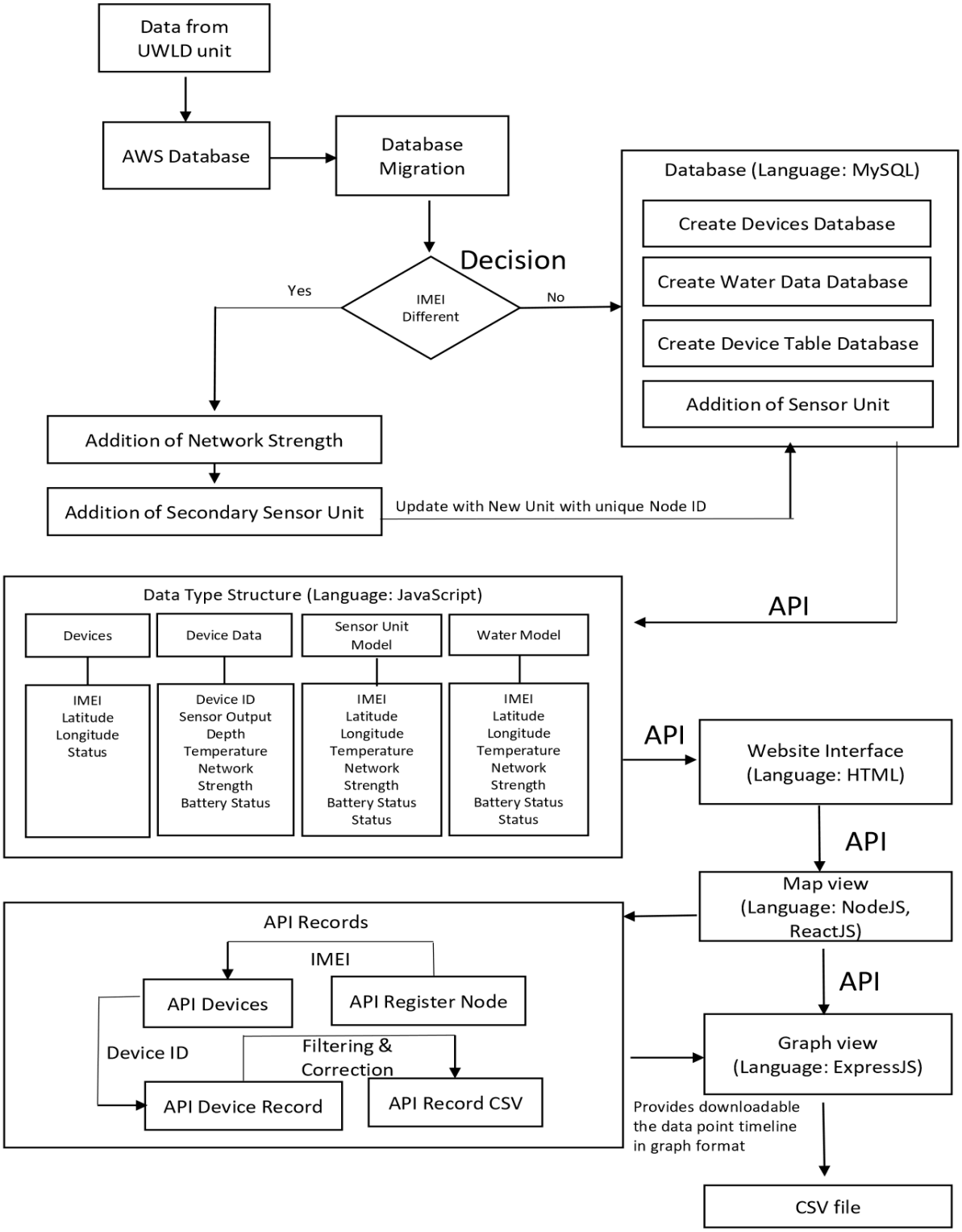

Figure 4. A flow chart of the AWS cloud data process algorithm.

3.2. UWLD system with dual MCU

Sleep mode is deployed in order to control the interval time after sending collected data to the server and before collecting data in the next cycle. However, the COP timer for a sleep mode presents inefficient energy-saving operation; due to the nature of the COP timer, the power is turned on and off every 8 to 10 seconds during the sleep mode regardless of the sleep time duration, and it makes to keep consuming the power while in the sleep mode (note Figure 5).

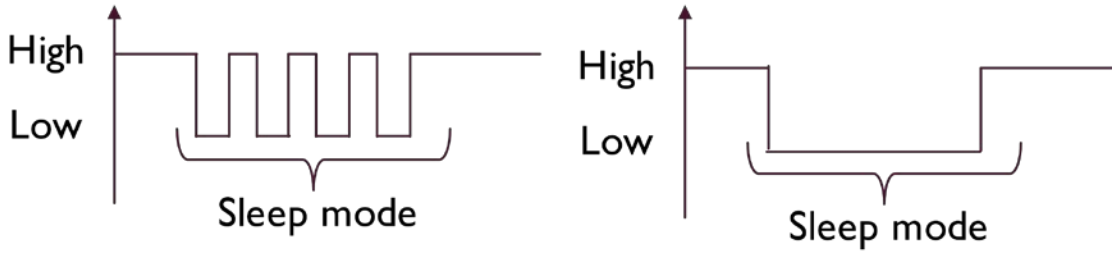

(a) (b)

Figure 5. Sleep mode operation with (a) COP timer and (d) ideal energy-saving mode

In addition, the basic sleep mode cannot control the real-time clock (RTC) or COP timer perfectly. Therefore, dual MCU is adopted to improve this inefficiency of the sleep mode by installing the additional MCU and solid-state relay (SSR), which has lesser power consumption. It would be anticipated that the total power consumption will have dwindled when the additional MCU is used as the alarm of the main MCU, which performs the main task, including measurement, calculation, and data transfer. The additional MCU is named as switch MCU because it exists only for turning on/off the main MCU. The connection of Dual MCU and relay in the UWLD system are shown in the flow chart of Figure 7. After transfer the data to AWS, the switch MCU turns off the main MCU and turns on again at the next interval time for data collection.

Two types of error prevention algorithms are employed. The first logic of the algorithm is to giving an operating time limit for 60 seconds. If data processes on the main MCU are incomplete in the limit, it means the error occurs during the cycle. So the main MCU should be turned off immediately and re-process data collection and transfer again without interval time. In case that the process is done within 60 seconds well, it means no error occurs and redo the process after the interval time. The second logic of the algorithm is to deployed a watchdog timer. The main MCU is turned off and on regularly, but in case of switch MCU, it will never be turned off. And it might cause a critical issue. That is the reason to use the watchdog timer to restart the switch MCU as well. The data process including the error prevention algorithm, is described in the flowchart of Figure 7. The design of PCB board is shown in Figure 8, which includes three main parts. Part A is the part for the switch MCU, part B is the part for a relay, and Part C is the part for the main MCU.

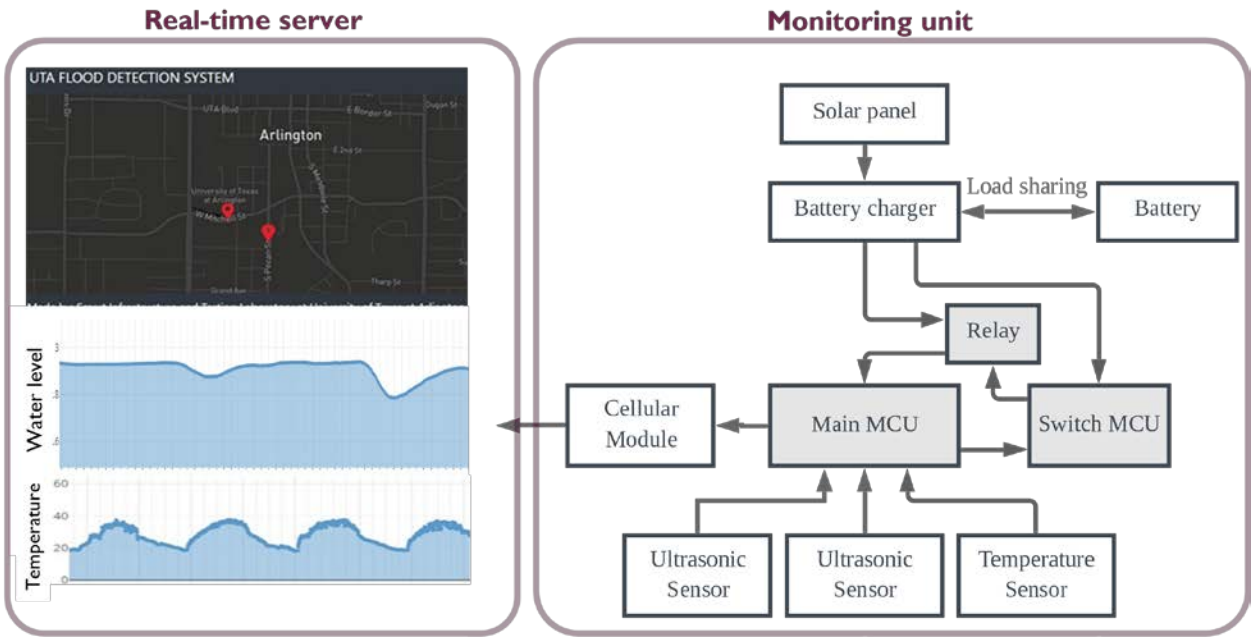

Figure 6. System representation of UWLD system; Dual target sensing and dual MCU

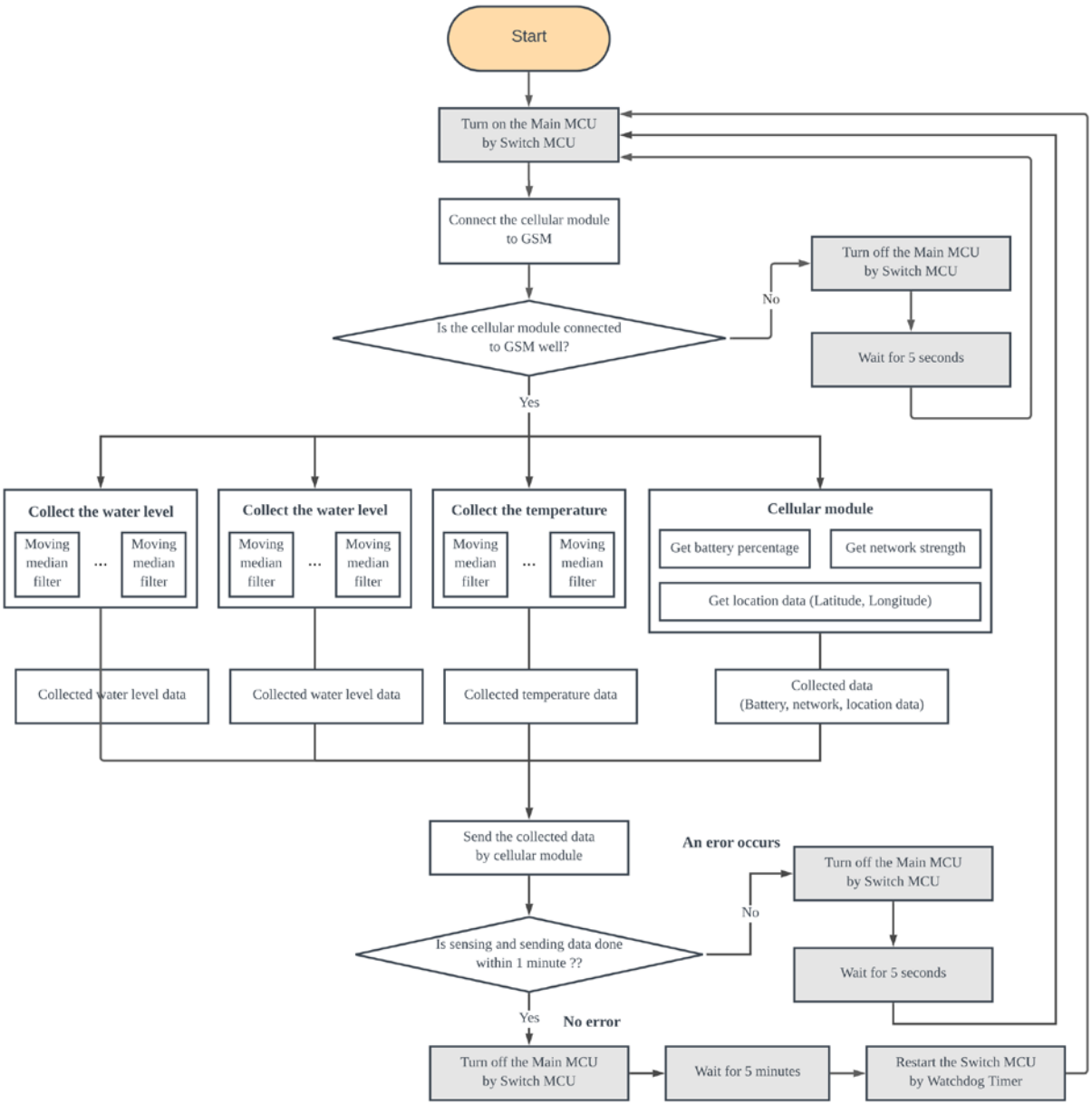

Figure 7. Flowchart of UWLD system; Dual target sensing and dual MCU

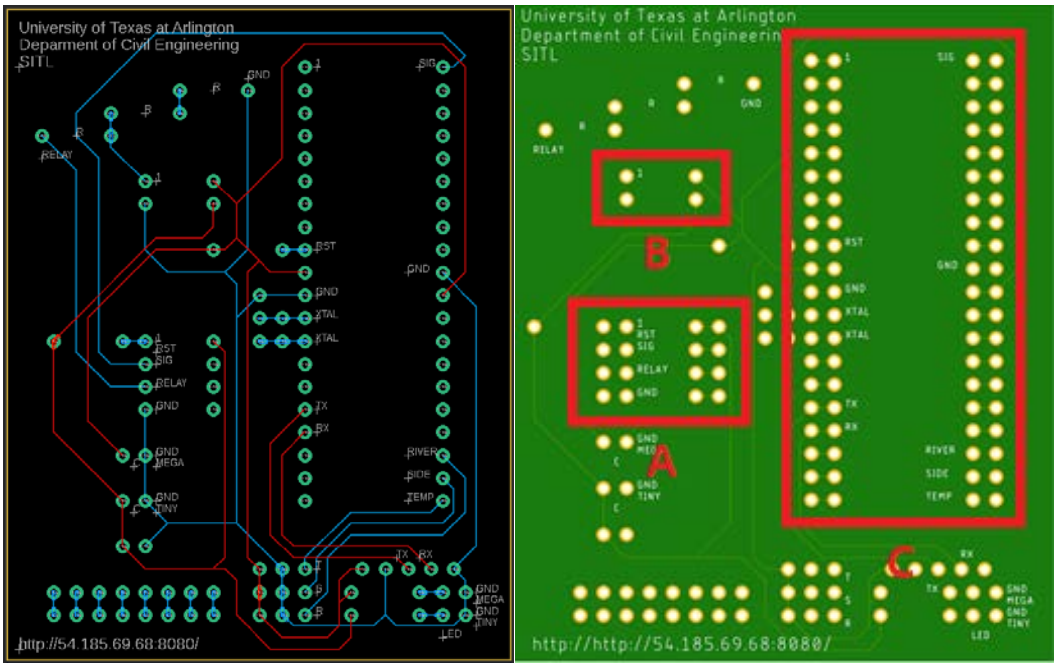

Figure 8. The final design of the UWLD system with Dual MCU system on PCB board

3.3. Dual target sensing with UWLD

Ultrasound sensors are deployed to calculate the distance between the sensor and the water surface. Water on the pavement could not only threaten the life of people but also damage the pavement surface when a flood occurs. So, it is highly important to sense both the water level on the streamside and on the pavement (see the additional sensor design in Figure 9 and Figure 10)

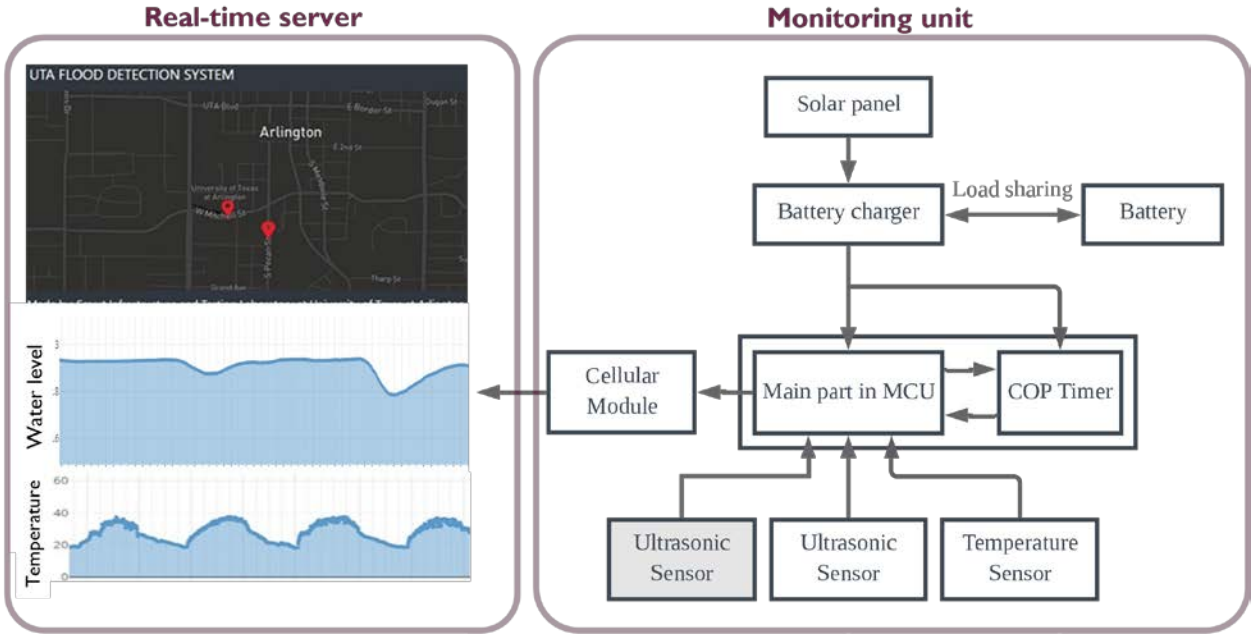

Figure 9. System representation of UWLD system 2; Dual target sensing

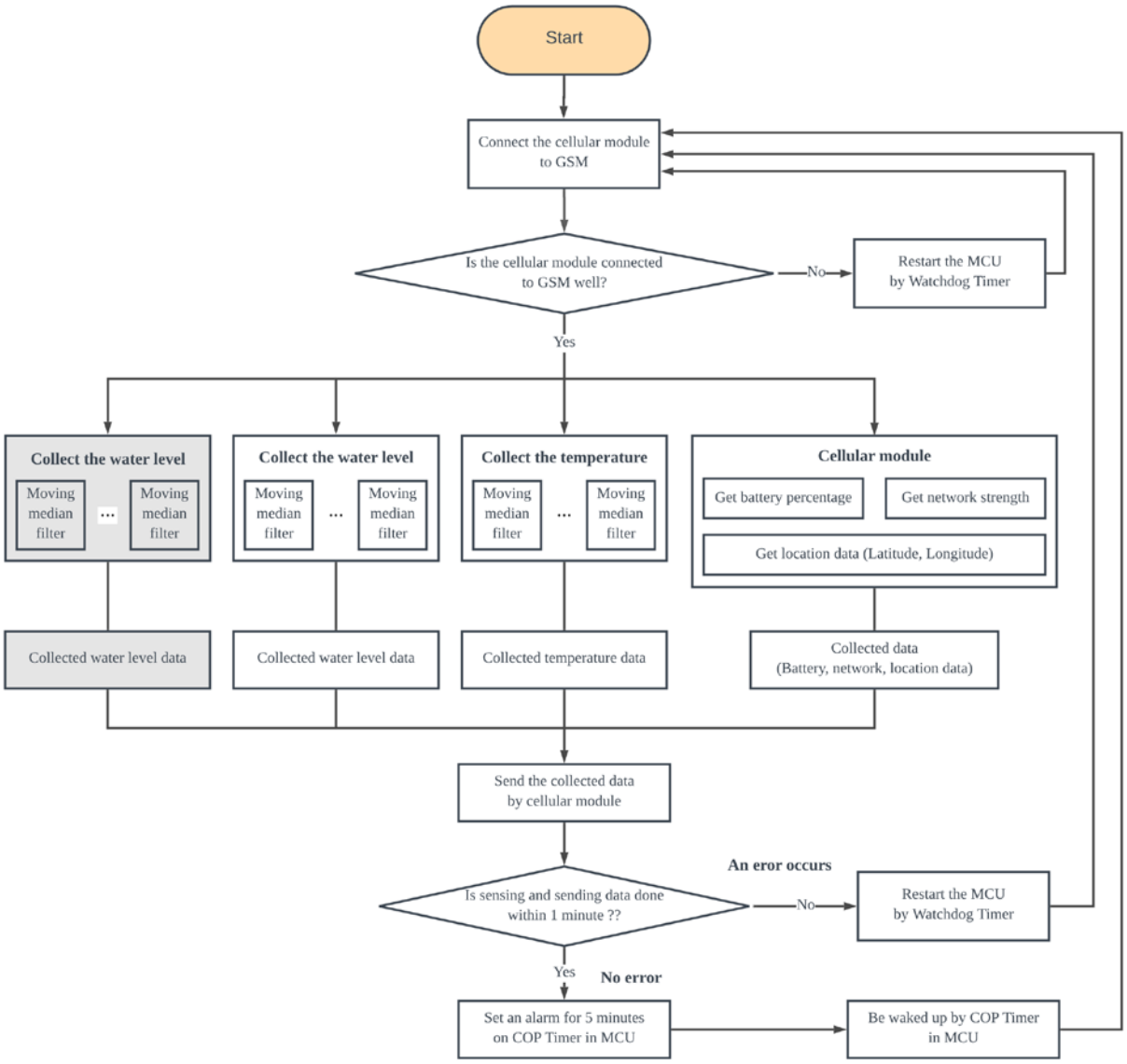

Figure 10. Flow chart of UWLD system with dual-target sensing

UWLD system nodes were installed at a local site near the University of Texas at Arlington (UTA). It is shown in Figure 11. One ultrasound sensor calculates the distance between the sensor and the water surface of the urban stream. And the other ultrasound sensor calculates the distance between the sensor and the water surface on the pavement when a flood occurs. The included temperature sensor will measure the temperature, which will be used for depth data revision on the server. The collected data will be sent to the AWS server by a cellular module. And these sensors and modules will be powered by a battery and a solar panel. The battery is in the enclosure, and the solar panel is placed on the enclosure.

Figure 11. Installed UWLD systems on site

4. FINDINGS

UWLD units have been installed near UTA, and they operate from late February utill August of 2020 for about six months. Two units were installed at two nodes, which does not hinder the public, and we did a regular system, and unit condition checks every week for the battery condition and sensor orientation. From March 1st 2020, data set were collected on the website and were periodically monitored until August 24th, 2020.

4.1. Preliminary Test of UWLD system

Figure 12. Modules were installed at the location at Node 1 and Node 2.

Two units of the UWLD system were installed at two locations, our local UTA site locations, Node 1 (N1), and Node 2 (N2). Node 1 was installed on February 17th, 2020, and Node 2 was installed on February 29th 2020, both these this installation was prioritized with respect to the forecast rainfall on the week ahead. The location is presented in the satellite view of the map in Figure 13.

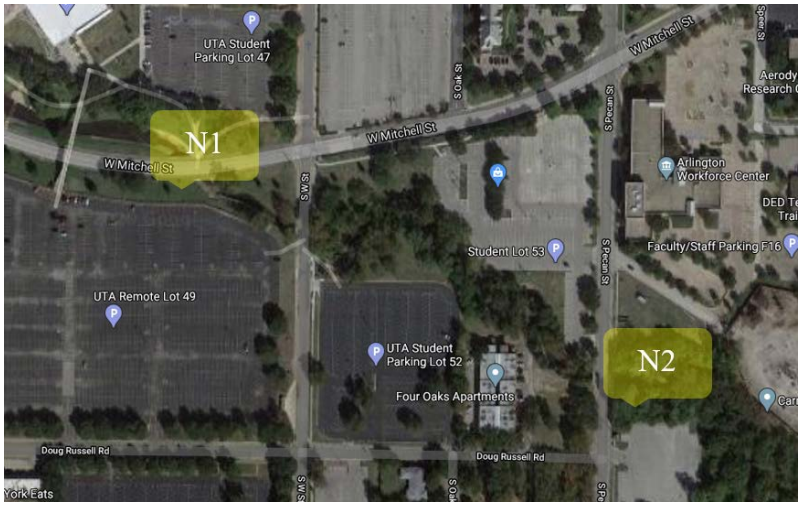

Figure 13. Satellite view of the site location

After installation, their respective heights of the sidewalk's ultrasound sensors of Node 1 and 2 where calibrated such that the sensor is placed at the minimum distance as per the requirement of the ultrasound sensor manual. Streamside sensors in both nodes are in the transducer performance range. Table 2 describes the height placed form the pavement level for the scanning.

Table 2. Sensor heights of the nodes at their locations, respectively.

Modules	Initial sensor height from the sidewalk (mm)	Initial sensor height from the stream (mm)
Node 1	700	3170
Node 2	640	3960

4.2. Verification Study of Water Level from the UWLD system

On completion of the installation, on-site tests were performed to check whether the sensor data provided were of accurate measure. Water level calibration tests require a container that is large enough such that it does not interfere with the ultrasound wave impulse sent from the sensor and be able to store water of 10-11 liters, which are required for measuring the change in water sensor level as shown in Figure 14. Calibration of sensor data, which considers the moving median and temperature correlation results were found to be a similar trend with the manual data measurements, as shown in Figure 15.

Calibration Procedure:

- Make sure the time interval of the water depth collection data is determined. For the current calibration test case, we considered 1 min and 5 min interval time
- Place the container in a position such that the center is in line with the sensor, and wait for the sensors to read the measurement.
- Fill the container with water to increase a few centimeters water level such it can be verified with manual measurement. The water level in the container is raised only at the in-between the time interval (5 min).
- Increase to the desired height of the water level is reached, and reading is recorded.

Figure 14. Water Level calibration test performed at nodes where container placed under the pavement sensor also manually measured readings with scale

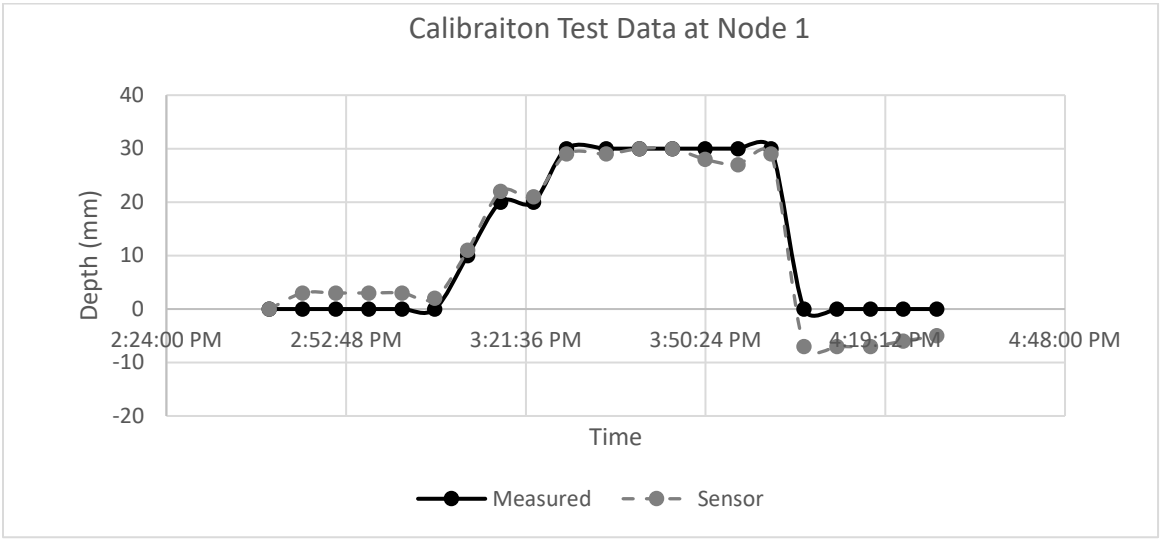

Figure 15. Water level calibration test for Node 1 where the blue line is verified with the manually measured data, and the red line represents the sensor measured data.

4.3. UWLD Rainfall Monitoring on Node 1 and 2

Once the calibration height has been set up for the nodes, the UWLD system has been collecting data since February. Collected sensor data have shown a good response with respect to the NOAA data at both the nodes. Rainfall data collected from our UWLD system which shows a rainfall with water level rise of 0.7 m and 0.6m at nodes 1 and 2 around 8 pm on March 15^{th,} 2020, as shown in Figure 16 and Figure 17. For the sidewalk, the ground level is considered zero levels whereas, on the stream, there is continuous water flow, so we considered an initial water depth level of 1m. NOAA recorded precipitation of 0.33 inch (8.382 mm) at Six Flag station on the same day. Also, at Lake Arlington, we can see the water level raise nearly an hour later than the period of rainfall as in Figure 18.

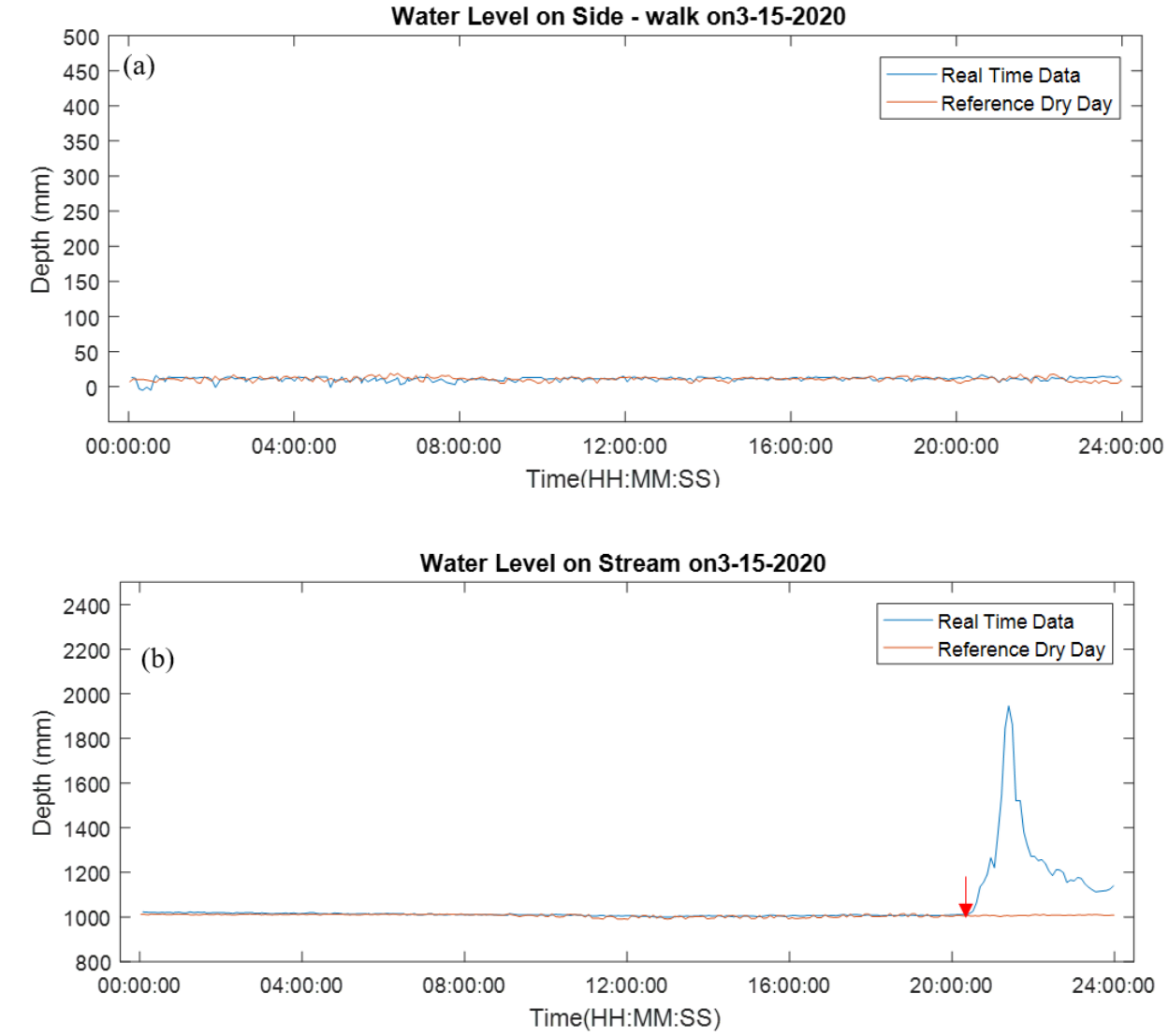

Figure 16. Precipitation data analysis of Node 1 for (a) Sidewalk Depth (b) Stream Depth.

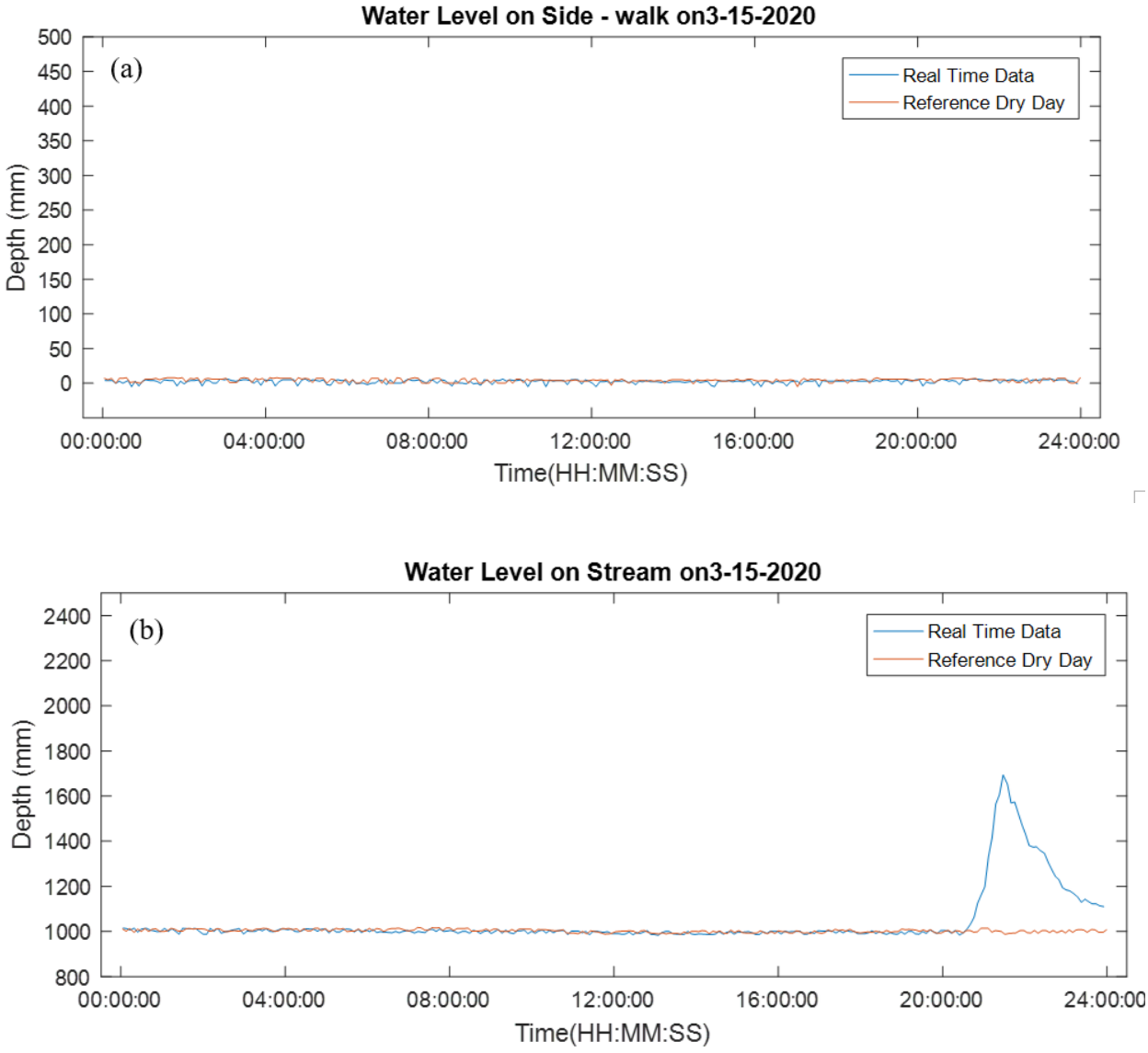

Figure 17. Precipitation data analysis of Node 2 for (a) Sidewalk Depth (b) Stream Depth.

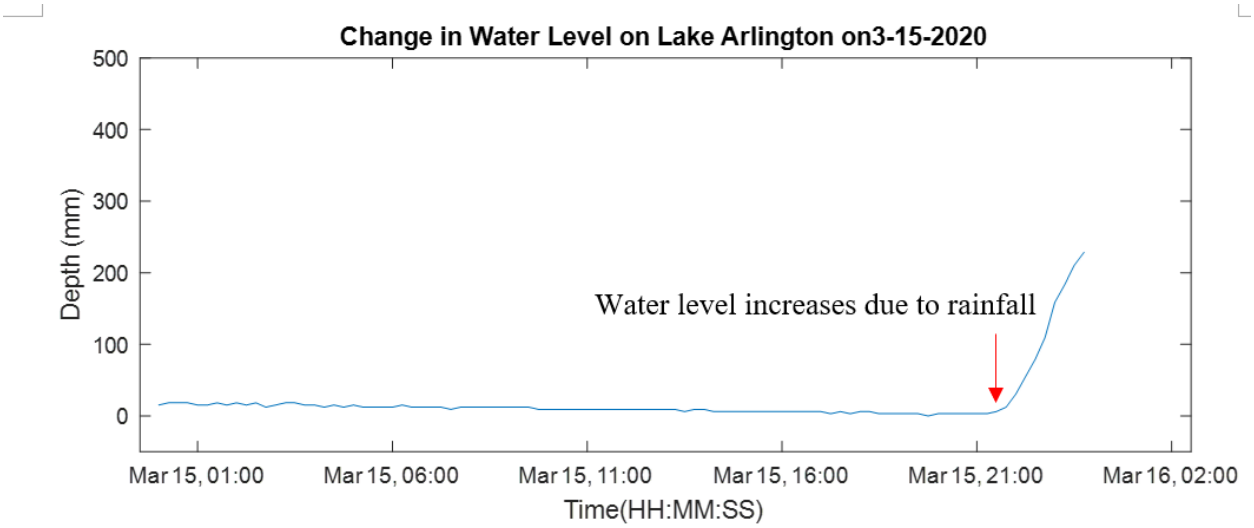

Figure 18. Precipitation data recorded at Lake Arlington.

On periodic monitoring, we found that the sidewalk of the bridges has a minimum water level raise due to the good drainage system of the bridge. But on a certain case, we found that the water level rise on the sidewalk of Node 1 due to the rainfall, which may be due to stagnation of water or any other obstacle in the side, which may lead to flash floods as shown in Figure 19. Whereas at Node 2 on the same day, we found the same level of water level rise in the streamside but a good drain of water at the sidewalk.

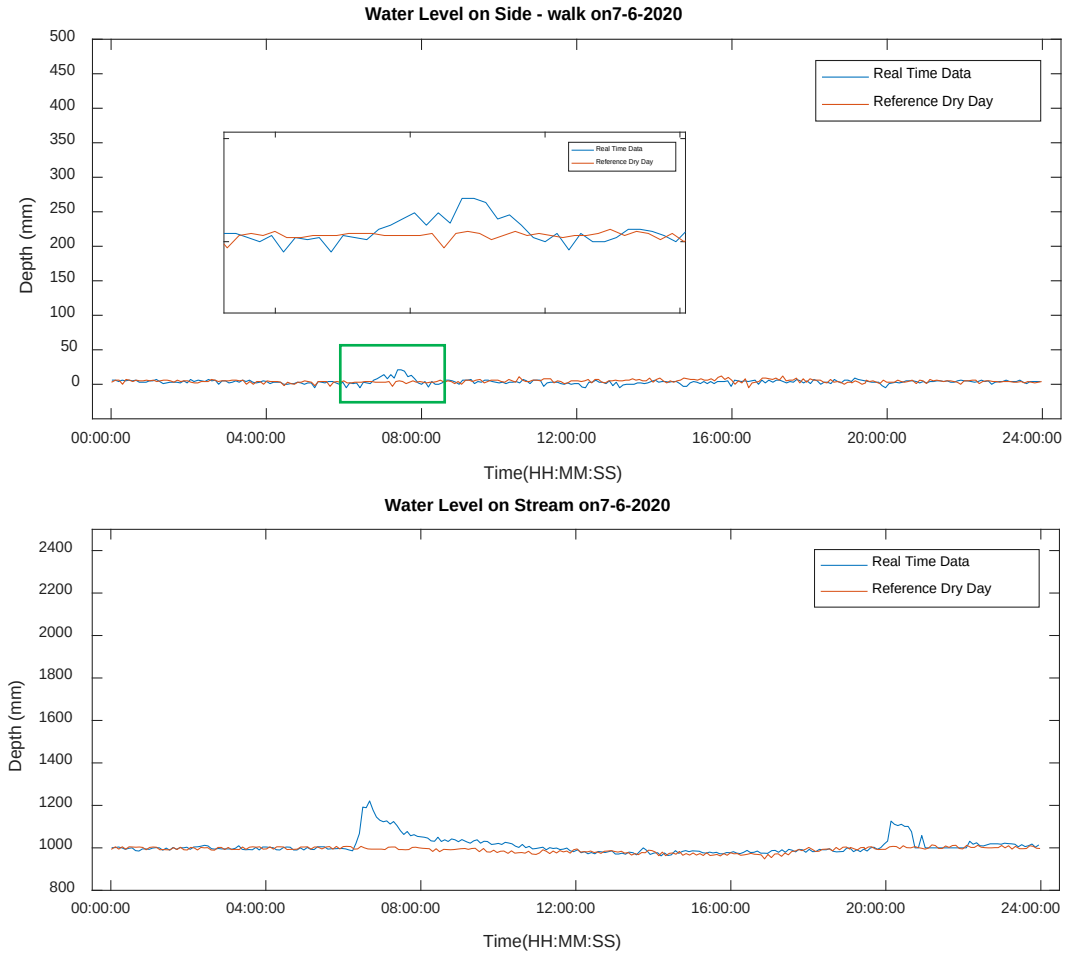

Figure 19. Water level raises recorded in the sidewalk location due to water staging at Node 1.

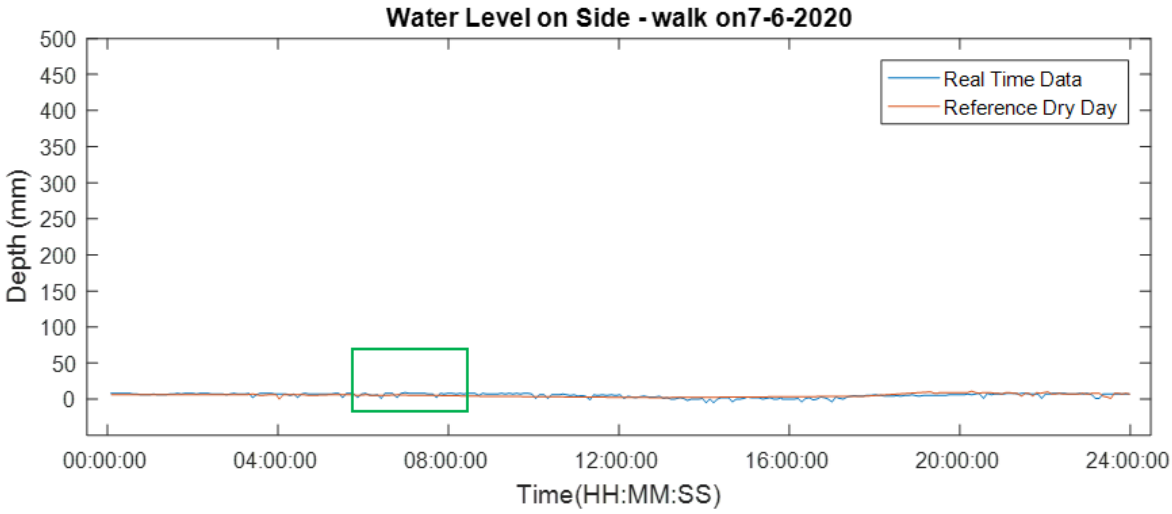

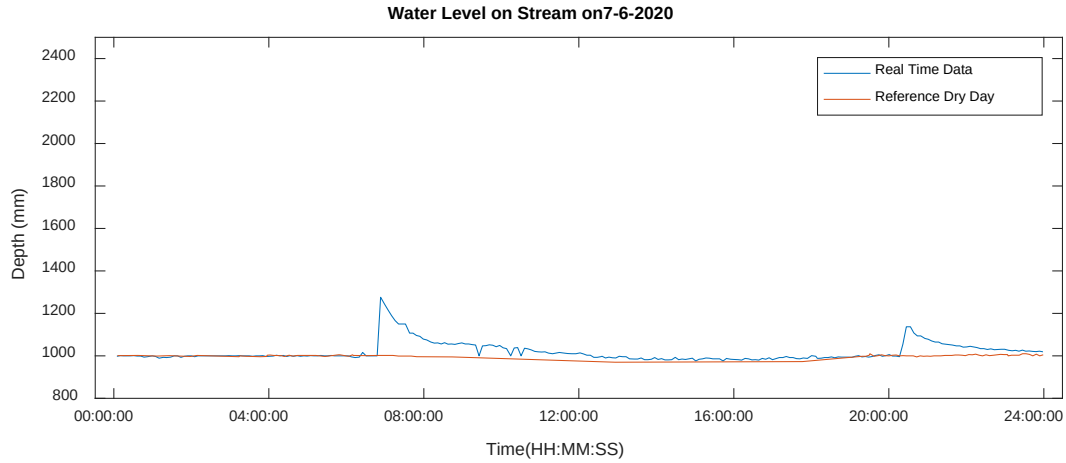

Figure 20. Water level with good drain recorded in the sidewalk location at Node 2 but the stream have a similar response to Node 1.

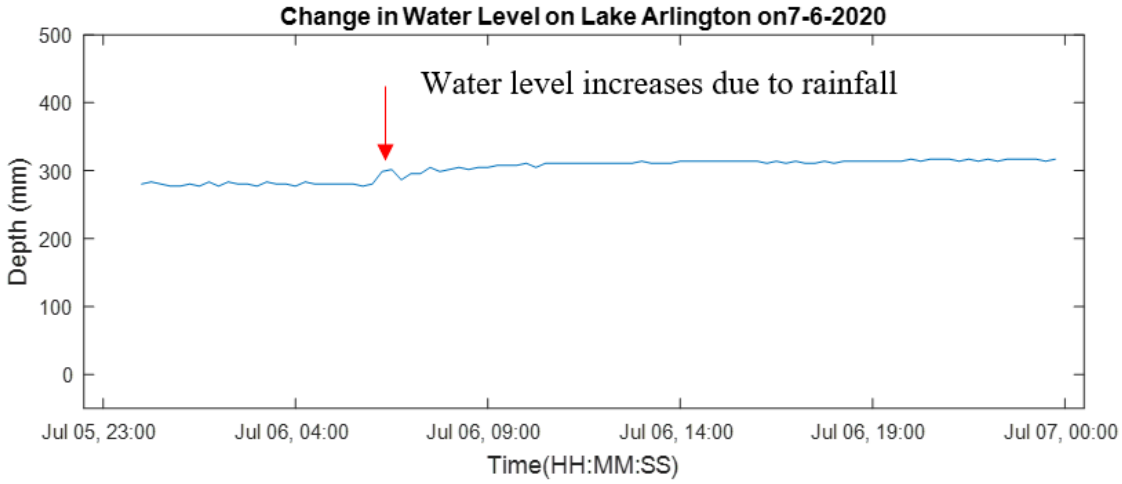

Figure 21. Precipitation data recorded at Lake Arlington.

Additional monitoring results in the rainy day are shown in Figure 22 and Figure 23. The figures show the water level changes on the streamside of Node 1 and Node 2 and Lake Arlington NOAA data.

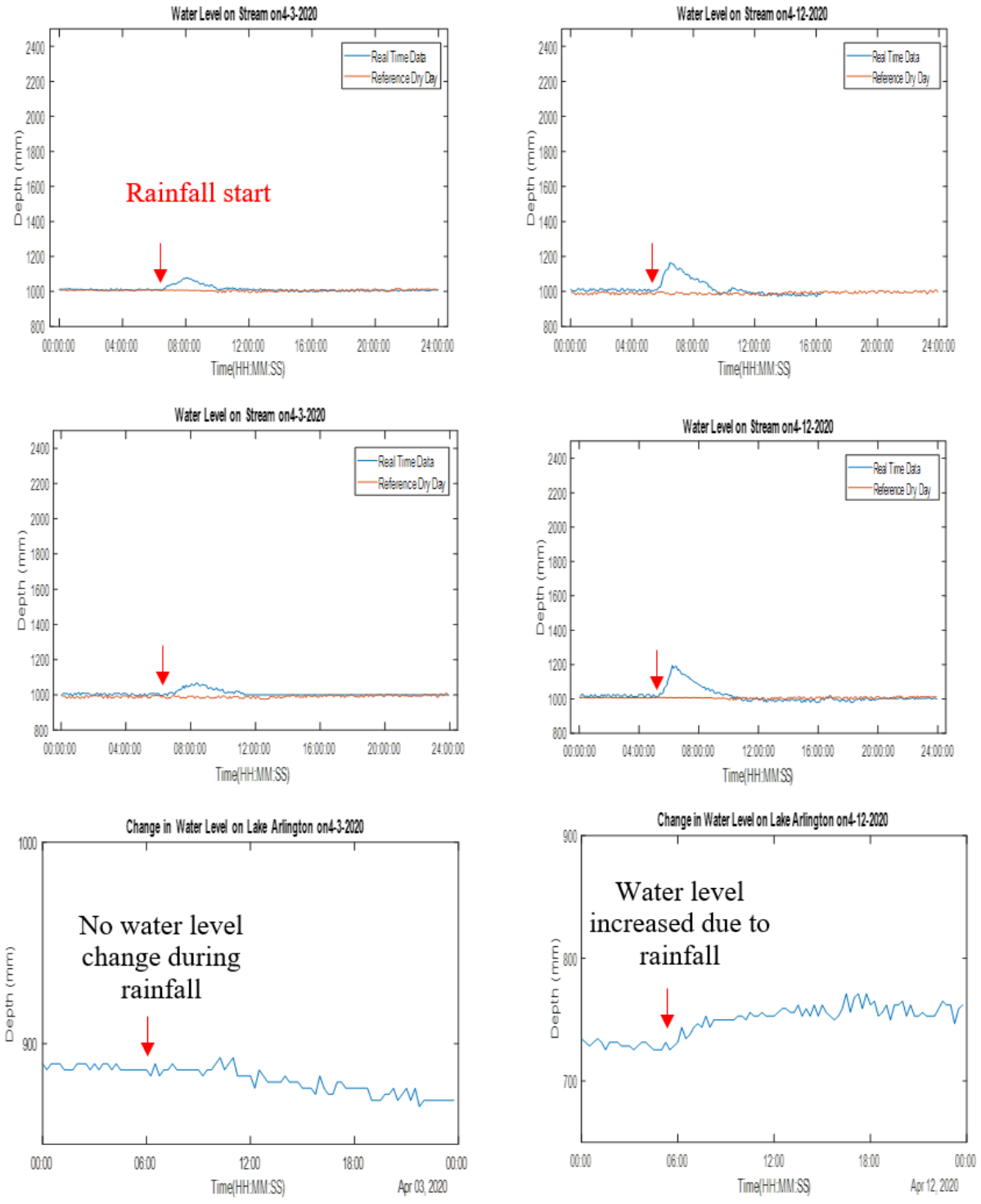

Figure 22. Precipitation data Collected from the stream side of Node1, Node 2 and Lake Arlington on (a) April 3rd (b) April 12th. It indicates that water level on the lake are less sensitive to detect rainfall data than the water level on the stream from UWLD system

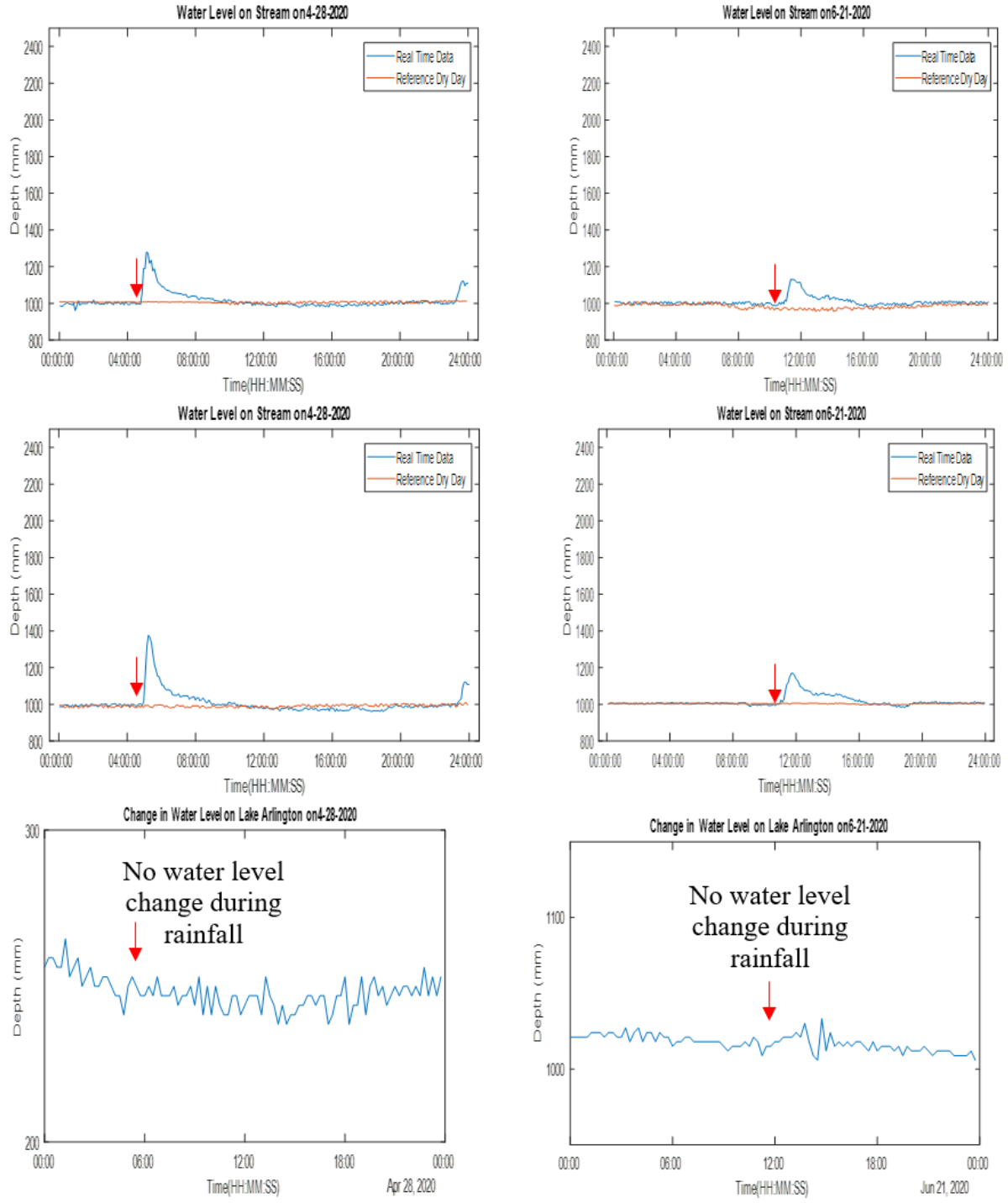

Figure 23. Precipitation data Collected from the streamside of Node1, Node 2 and Lake Arlington on (a) April 28th (b) June 21st

Figure 24 shows the scattered peak water level data of 16 rainy days obtained by monitoring the water level for six months. Water level peak values from the UWLD system on the streamside and

Lake Arlington NOAA data are considered to plot the data. The scatter plot indicates some cases of streamside and lake water levels present strong correlation during a rainy day, while in most case the lake water level is not always increasing as streamside water level increases due to their different environment. The water level on streamside sensitively responds.

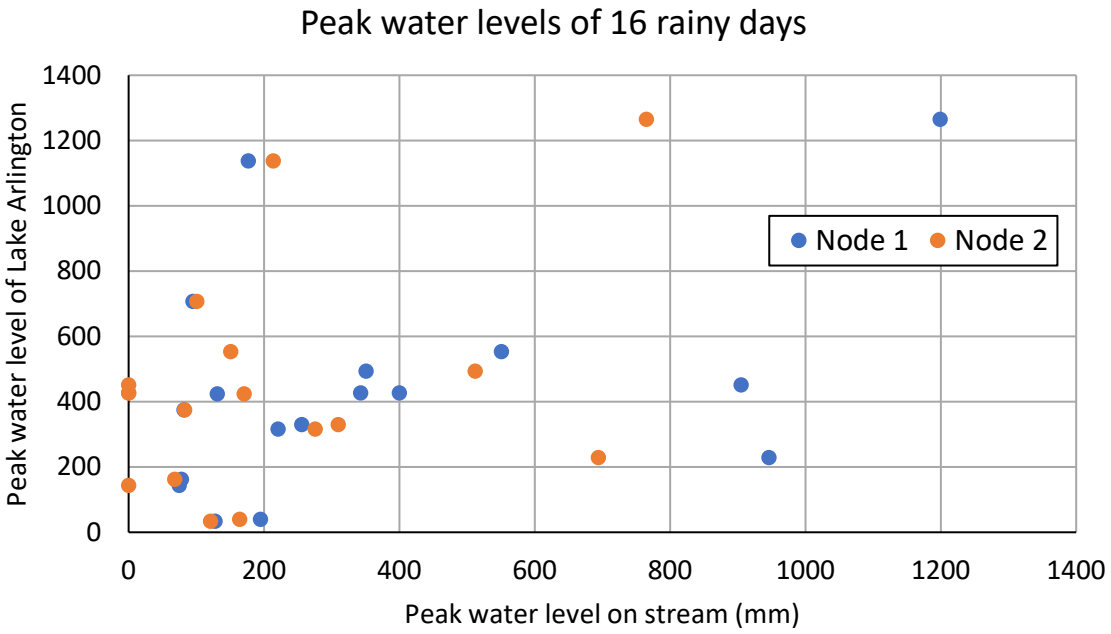

Figure 24. Scatter plot of the peak water level data from nodes stream data and Lake Arlington NOAA data

4.4. Energy efficiency of the UWLD system

Apart from data collection analysis, we have encountered few maintenance issues like power shortage due to the shady location of the UWLD system—the efficiency of the battery power supply with dual microcontrollers (Dual MCUs).

It is essential for the UWLD system to be functional during the rainy season as to monitor the water level during that period. If it runs out of battery power and gets turned off, the system objective has not been attained. So it is necessary to consider how much battery is consumed due to the solar panel and when the solar panel does not charge the battery. We considered a 36 hour time period of the batter power usage, which has the battery power drained during the day and replacement of the battery the next day, shown in Figure 25; Part A is night time, and Part B is in the day time. As shown in the figure, even in the day time, the charging rate is lower than power consumption.

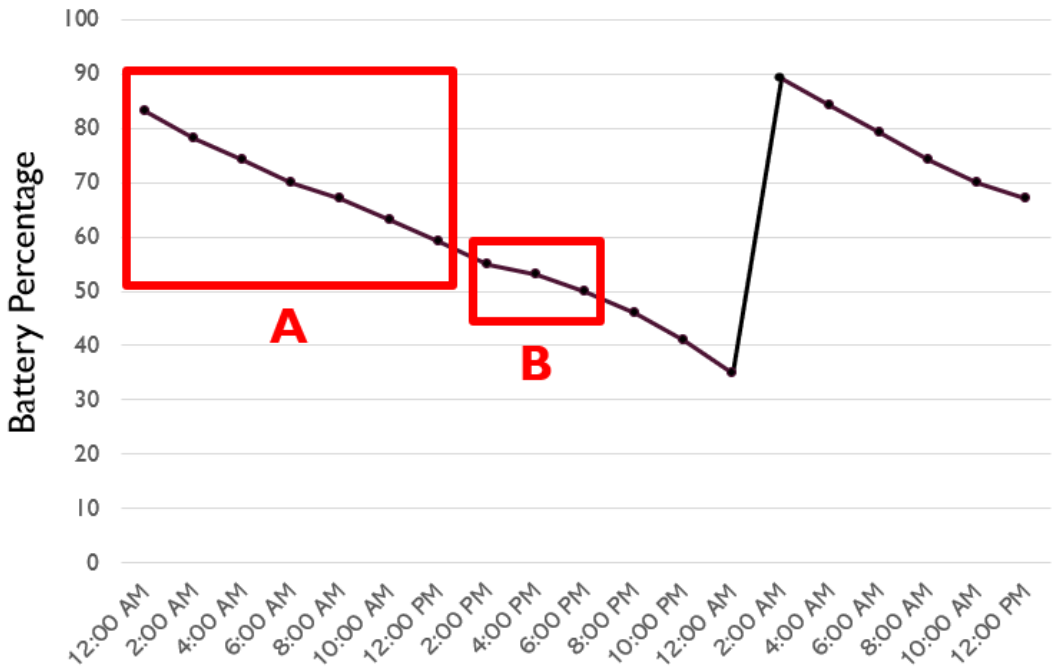

Figure 25. Monitoring of the battery percentage for 36 hours.

Battery change operation from February 19th 00:00 am to February 20th at 12:00 pm, which is represented as two boxes are marked on the graph. Part A covers from February 19th, 00:00 am to February 19th 12:00 pm. It shows the battery consumption during the time when the sunlight is absent or not strong to charge the battery. And it shows a rapid drop of 24% battery percentage from 83% to 59% for 12 hours. Part B covers from 2:00 pm to 6:00 pm. It shows the battery consumption during the daytime when the sunlight is strong enough to charge the battery. But it shows only a lesser drop of 5% from 55% to 50% for 4 hours. Despite considering the cloudy weather, the battery consumption and battery charging rate should be improved. Unless they are improved, the system would end up turned off unintentionally, which harms the trust of UWLD system.

4.5. Dual Microcontroller of the UWLD system

Since UWLD system has a problem in battery sustainability, though it is important to keep the system working in cloudy weather, the battery usage drop is significant than battery charging which leads shut down of the system. So the analysis on battery consumption of the system is conducted shown in Figure 26. Battery consumption of each module is measured with the help of a multi-meter which showed that the MCU runtime has the biggest consumption and sleep mode break time as an additional problem of power consumption, which accounts for 110 mA and 50 mA respectively. In-addition to Dual MCU, change of main MCU should be employed as well.

The MCU model should be chosen based on actual trial-and-error method. Because a MCU having small size of data memory SRAM and flash memory normally consumes less power. But if we consider a MCU which has a smaller size SRAM and flash memory, it could not run the code

sustainably. So, a list of MCU models is made first, and the most appropriate MCU should be chosen on a trial-and-error basis. Finally the MCU having smallest size of SRAM and flash memory would be chosen, which should be able to run the code sustainably.

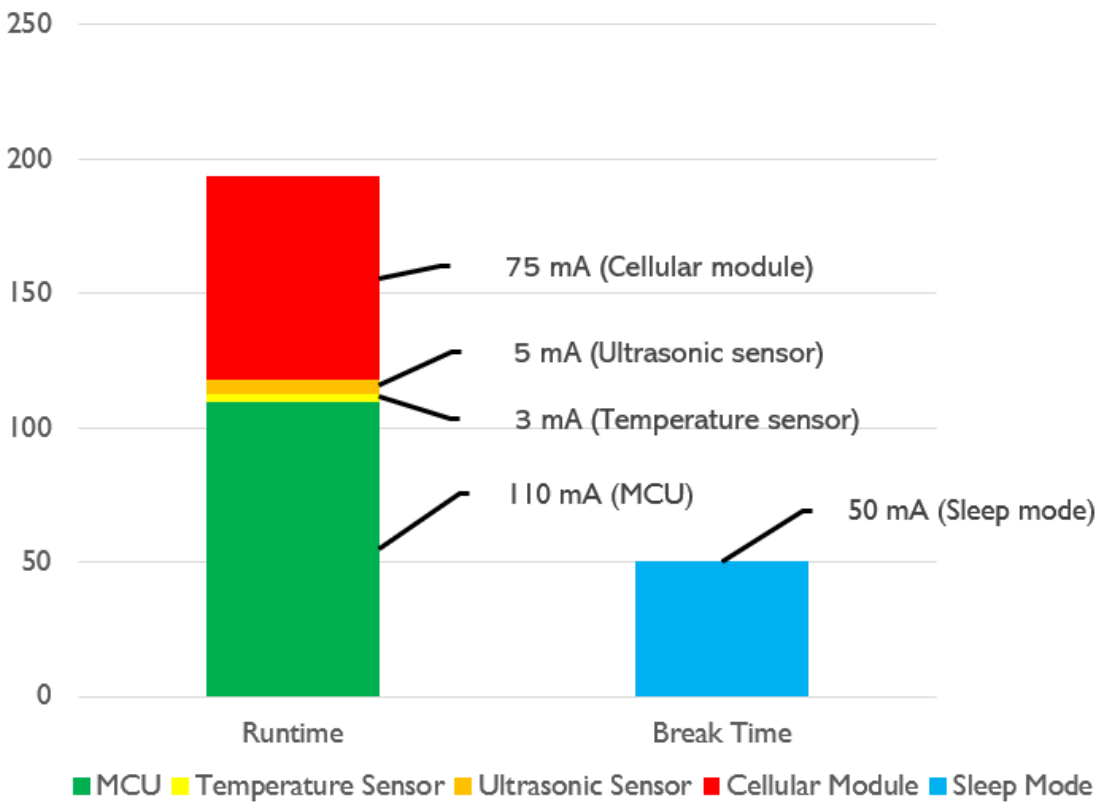

Figure 26. Battery consumption by each module

After employing Dual MCU and deploying the appropriate MCU model through trial-and-error, similar 36 hours of operation test was done again, which covers 36 hours operation from April 12th 00:00 am to April 13th at midnight. And the battery change graph comparison is described in Figure 27.

Here we can infer in Part A for a time period from 00:00 am to 12:00 pm, which shows the lesser battery consumption when the sunlight is absent or not strong enough to charge the battery. And the time on the x-axis means the same time on both February 19th and April 12th, so 00:00 am means 00:00 am on February 19th and April 12th both. UWLD system showed a rapid drop percentage of 24% from 83% to 59%, but the UWLD system with Dual MCU shows a lesser drop percentage of 13% from 85% to 72%. Also, in Part B for the time period from 2:00 pm to 6:00 pm shows that charging of battery when the sunlight is strong enough even though the UWLD system consumes the battery. Previous UWLD system shows drop percentage of 5% from 55% to 50% for 4 hours, but current UWLD system with Dual MCU shows a percentage increase of 14% from 72% to 86%.

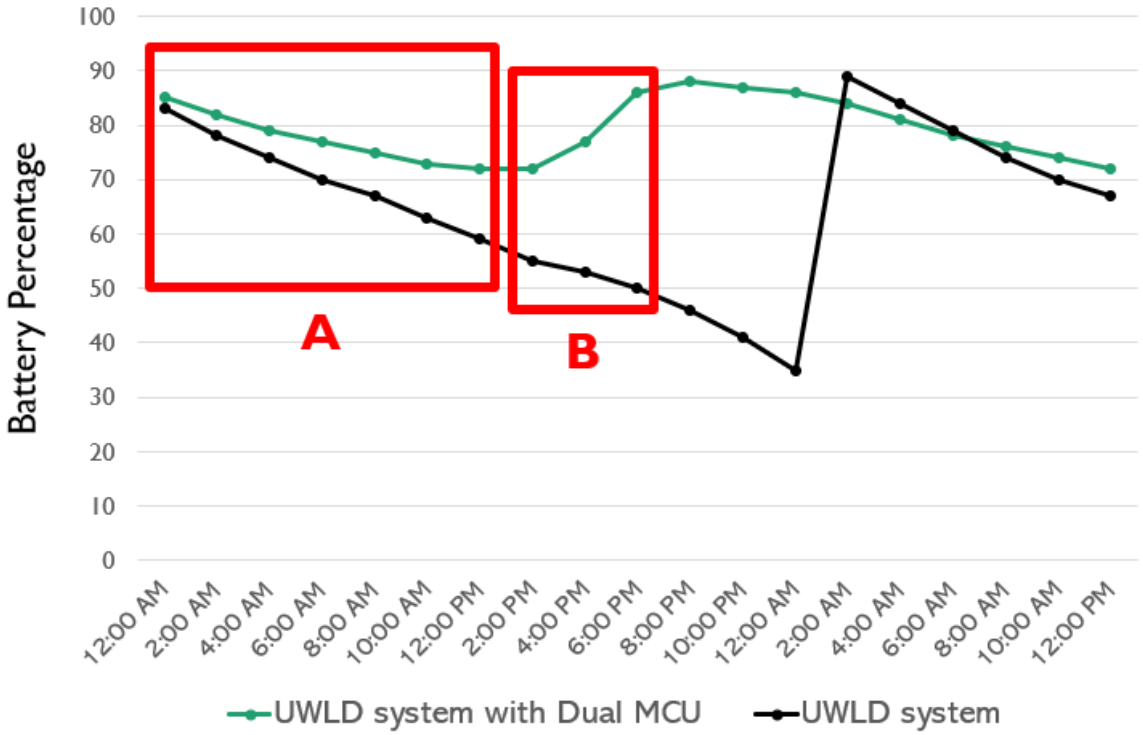

Figure 27. 36 hours battery percentage record comparison

As described above, employing dual MCU makes a marked improvement on the battery percentage drop during the time when the sunlight is absent or not strong enough to charge the battery. The measured current by a multi-meter is shown in Figure 28. The average current consumed during the runtime was 165 mA, and it is have reduced consumption of roughly 110 mA. The current during the interval time was 50 mA, and have reduced consumption of 15mA. This remarked improvement in the efficient sustainable current flow of the circuitry system, which results in more effective battery consumption shown above.

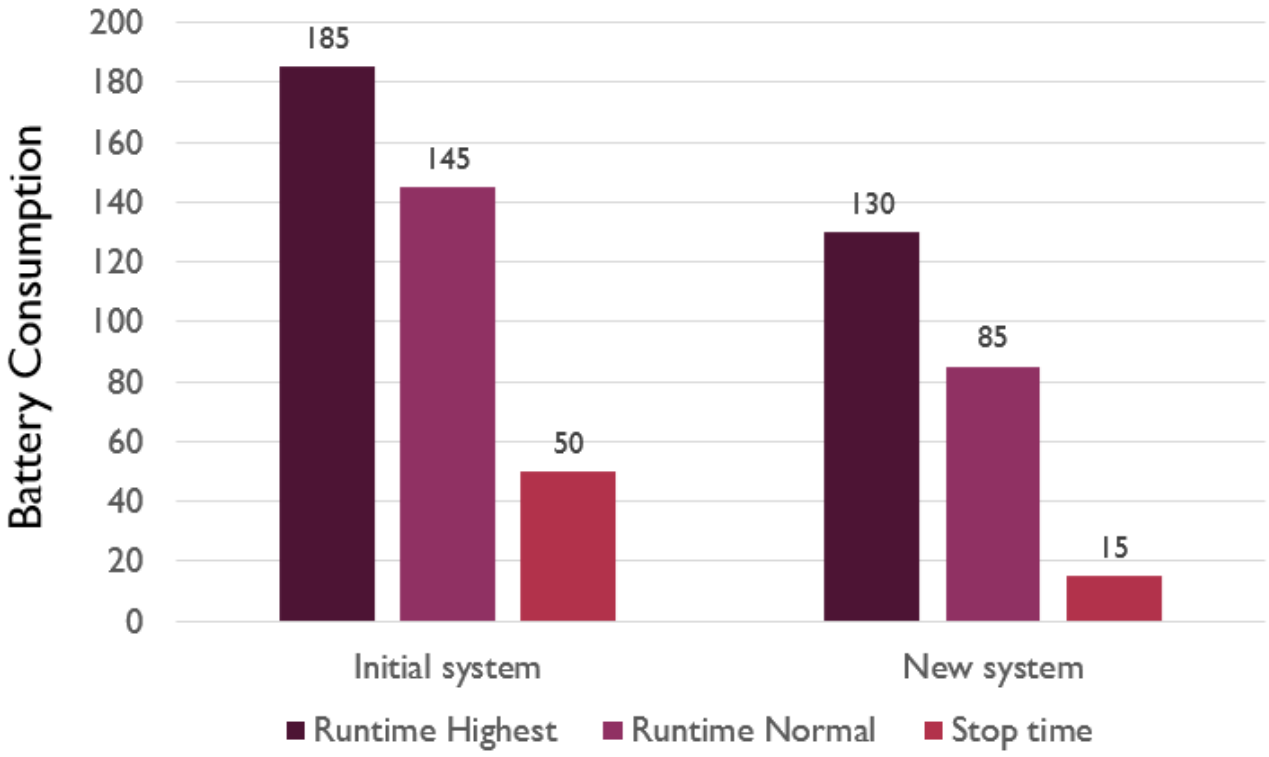

Figure 28. Battery consumption comparison

4.6 CONCLUSIONS

The real-time water level monitoring was conducted with the measured data by the developed UWLD system and real-time monitoring system through AWS. Dual MCU system was considered to build the efficient power supply and consumption, and dual targets of the water level detection are considered to study the relationship between the water level change by the targets in different amount and duration of rainfall.

- The UWLD system was developed to measure the water level and transfer the data to the AWS server; the obtained water level is calibrated with the ultrasound wave velocity change by the temperature. In addition, the accuracy of the distance measurement was verified with manually measured distance.

- From the UWLD system, a total of 16 water level changes were detected for six month monitoring period (March 1st to August 24th, 2020). When the streamside water level increases from our UWLD system, the lake water level from NOAA data did change or increased later, it implies the water level change at local small creek or stream is more sensitive flood level indicator than at the large water bodies (e.g., lake or sea level). It is a challenge to monitor flood levels at the lake because of its low sensitivity environment. Thus, it is significant to perceive the intensity of the rainfall from streamside

- The water level change on the pavement side is not always detected as streamside water level change due to the good drainage system. Among 32 cases of the monitoring water level on the pavement side, only 3 cases (March 16th, 18th, and July 6th) presents the pavement side water level changes during the rainfall at the Node 1 location. Although the pavement side water level changes are more affected by infrastructure conditions (e.g., the drainage system) then the direct rainfall intensity, it can be more significant to warn the urban flooding, especially close to the area of UWLD station. Therefore, the water level monitoring of dual targets, pavement side, and streamside, can give more reliable and sensitive information to perceive and forecast the urban flash flooding.

- The battery power efficiency was improved for the stable operation of the UWLD system deploying the dual MCU unit, which is composed of the additional MCU (switch MCU) and SSR for controlling the main MCU. The dual MCU system reduced the power consumption from 165 mA to 110 mA of the averaged current consumption. It is significant for the power saving during solar power charging which is affected by the external environment (e.g., rainfall and cloudy day)

REFERENCES

1. French, J., R. Ing, S. Von Allmen, and R. Wood. Mortality from Flash Floods: A Review of National Weather Service Reports, 1969-81. *Public health reports (Washington, D.C. : 1974)*, Vol. 98, No. 6, 1983, pp. 584–8.

2. Ben Cave, Liza Cragg, Jo Gray, P. D. P., and S. T. Katherine Pygott. *Understanding of and Response to Severe Flash Flooding*. Almondsbury, Bristol, 2017.

3. Lal, R., A. Shanwal, and S. Singh. Remote Sensing and GIS Applications in Watershed Management. *Encyclopedia of Soil Science, Second Edition*, No. January, 2010. https://doi.org/10.1201/noe0849338304.ch308.

4. Caroline A. Mays. Texas Freight Mobility Plan 2017. *TxDOT*. 364.

5. Mousa, M., and C. Claudel. Poster Abstract: Water Level Estimation in Urban Ultrasonic/Passive Infrared Flash Flood Sensor Networks Using Supervised Learning. *IPSN 2014 - Proceedings of the 13th International Symposium on Information Processing in Sensor Networks (Part of CPS Week)*, 2014, pp. 277–278. https://doi.org/10.1109/IPSN.2014.6846761.

6. Sakharov, V. E., S. A. Kuznetsov, B. D. Zaitsev, I. E. Kuznetsova, and S. G. Joshi. Liquid Level Sensor Using Ultrasonic Lamb Waves. *Ultrasonics*, Vol. 41, No. 4, 2003, pp. 319–322. https://doi.org/10.1016/S0041-624X(02)00459-6.

7. Basha, E. A., S. Ravela, and D. Rus. Model-Based Monitoring for Early Warning Flood Detection. *SenSys'08 - Proceedings of the 6th ACM Conference on Embedded Networked Sensor Systems*, 2008, pp. 295–308. https://doi.org/10.1145/1460412.1460442.

8. Mousa, M., X. Zhang, and C. Claudel. Flash Flood Detection in Urban Cities Using Ultrasonic and Infrared Sensors. *IEEE Sensors Journal*, Vol. 16, No. 19, 2016, pp. 7204–7216. https://doi.org/10.1109/JSEN.2016.2592359.

9. Bies, D. A., and C. H. Hansen. *Engineering Noise Control - Theory and Practice*. CRC Press, New York, 2009.

10. Ham, S., H. Song, M. L. Oelze, and J. S. Popovics. A Contactless Ultrasonic Surface Wave Approach to Characterize Distributed Cracking Damage in Concrete. *Ultrasonics*, Vol. 75, 2017, pp. 46–57. https://doi.org/10.1016/j.ultras.2016.11.003.

11. Ham, S., and J. S. Popovics. Application of Micro-Electro-Mechanical Sensors Contactless NDT of Concrete Structures. *Sensors (Switzerland)*, Vol. 15, No. 4, 2015, pp. 9078–9096. https://doi.org/10.3390/s150409078.

12. Sun, H., S. M. Asce, J. Zhu, A. M. Asce, and S. Ham. Automated Acoustic Scanning System for Delamination Detection in Concrete Bridge Decks. Vol. 23, No. 6, 2018, pp. 1–9. https://doi.org/10.1061/(ASCE)BE.1943-5592.0001237.

13. Johnston, F. R., J. E. Boyland, M. Meadows, and E. Shale. Some Properties of a Simple Moving Average When Applied to Forecasting a Time Series. *Journal of the Operational Research Society*, Vol. 50, No. 12, 1999, pp. 1267–1271. https://doi.org/10.1057/palgrave.jors.2600823.

14. Stone, D. C. Application of Median Filtering to Noisy Data. *Canadian Journal of Chemistry*, Vol. 73, No. 10, 1995, pp. 1573–1581.

15. Sadler, J. M., D. P. Ames, and R. Khattar. A Recipe for Standards-Based Data Sharing Using Open Source Software and Low-Cost Electronics. *Journal of Hydroinformatics*, Vol. 18, No. 2, 2016, pp. 185–197. https://doi.org/10.2166/hydro.2015.092.

16. Rompas, P. S., and A. A. Wardana. Robust Flood Monitoring Platform Using Message Queueing Telemetry Transport Protocol. *2017 International conference on information technology systems and innovation (ICITSI)*, 2017, pp. 234–238.

17. Frolov, A. V., V. V. Asmus, S. V. Borshch, R. M. Vil' fand, I. I. Zhabina, V. V. Zatyagalova, V. A. Krovotyntsev, O. I. Kudryavtseva, E. A. Leont' eva, Y. A. Simonov, and Y. A. Stepanov. GIS-Amur System of Flood Monitoring, Forecasting, and Early Warning. *Russian Meteorology and Hydrology*, Vol. 41, No. 3, 2016, pp. 157–169. https://doi.org/10.3103/S1068373916030018.